FACULDADE DE ENGENHARIA DA UNIVERSIDADE DO PORTO

Measurement System for Evaluation of Cycling Performance

Diogo José Fernandes Gonçalves

DISSERTATION

Mestrado em Engenharia Biomédica

Supervisor: Miguel Velhote Correia

October 1, 2017

© Diogo José Fernandes Gonçalves, 2017

U.PORTO
FEUP FACULDADE DE ENGENHARIA
UNIVERSIDADE DO PORTO

MEB - MESTRADO EM ENGENHARIA BIOMÉDICA **2016/2017**

A Dissertação intitulada

"Measurement System for Evaluation of Cycling Performance"

foi aprovada em provas realizadas em 20-10-2017

o júri

Presidente Prof. Doutor Joaquim Gabriel Magalhães Mendes
Professor Auxiliar do Departamento de Engenharia Mecânica da FEUP - U.Porto

Prof. Doutor Miguel Fernando Paiva Velhote Correia
Professor Auxiliar do Departamento de Engenharia Eletrotécnica e de Computadores da FEUP - U. Porto

Prof. Doutor Lino Manuel Baptista Figueiredo
Professor Adjunto do Instituto Superior de Engenharia do Porto do Instituto Politécnico do Porto

O autor declara que a presente dissertação (ou relatório de projeto) é da sua exclusiva autoria e foi escrita sem qualquer apoio externo não explicitamente autorizado. Os resultados, ideias, parágrafos, ou outros extratos tomados de ou inspirados em trabalhos de outros autores, e demais referências bibliográficas usadas, são corretamente citados.

Diogo José Fernandes Gonçalves
Autor - Diogo José Fernandes Gonçalves

Faculdade de Engenharia da Universidade do Porto

Measurement System for Evaluation of Cycling Performance

Diogo José Fernandes Gonçalves

Mestrado em Engenharia Biomédica

October 1, 2017

Resumo

O ciclismo é um desporto com cada vez mais admiradores e praticantes em todo o mundo, e devido a isso, temos assistido a um aumento de interesse nesta modalidade desportiva. O uso de sistemas auxiliares para melhorar as metodologias de treino e, consequentemente, melhorar a técnica e o desempenho no ciclismo seria de extrema importância para atletas e treinadores.

O objetivo deste estudo foi desenvolver um sistema de monitorização para o ciclismo. O sistema desenvolvido é composto por duas entidades: dispositivos físicos que devem recolher, armazenar e enviar os dados lidos pelos sensores e um smartphone que funciona como uma interface de visualização. A transmissão entre estas duas entidades é realizada através da tecnologia de comunicação sem fios Bluetooth Low Energy.

Um conjunto de testes experimentais foram realizados com um atleta de modo a avaliar seu posicionamento na bicicleta e o seu movimento de pedalagem. Os nodos sensoriais do sistema foram posicionados no membro inferior direito do atleta, nomeadamente na coxa e na perna. Foram recolhidos os valores dos ângulos de Euler de cada dispositivo, de modo a obter o ângulo do joelho resultante ao longo do percurso.

A implementação deste sistema permitiu um feedback em tempo real e uma análise pós-treino mais detalhada, funcionando como uma ferramenta de suporte para o atleta ser capaz de optimizar o seu desempenho no ciclismo.

Abstract

Cycling is a sport with increasingly admirers and practitioners all over the world, and due to that, there have been an interest boost on this sport modality. The use of auxiliary systems to improve training methodologies and consequently enhance cycling technique and performance would be extremely important for athletes and coaches.

The goal of this study was to develop a measurement system for cycling. This system is composed by two entities: physical devices that must collect, store and send the data read by the sensors and a smartphone that works as a display interface. Transmission between these two entities is performed via wireless communication based on Bluetooth Low Energy technology.

A set of experimental tests were performed with an athlete in order to evaluate his positioning on the bicycle and its pedaling movement. The system's sensory nodes were positioned on the right lower limb of the athlete, namely in the thigh and shank. The Euler angles values of each device were collected in order to obtain the resulting knee angle along the trials.

The implementation of this system allowed a real-time feedback and a more detailed post-training analysis, functioning as a support tool for the athlete be able to optimize his cycling performance.

Acknowledgements

First of all I would like to thank to my supervisor, Professor Miguel Velhote Correia for helping me whenever I need and for sharing their knowledge and experience with me.

Secondly, my thanks to the other professors and technicians of the Faculty of Engineering of the University of Porto, who contributed to the implementation of this dissertation.

A special thanks to all my colleagues and friends for their help and support throughout this journey.

A special mention to the athlete Luis Santos, for the availability demonstrated in the accomplishment of the experimental tests.

And finally, I am deeply grateful to my family, for the confidence and support provided in all phases of my academic journey, because without them this route would not be possible.

Diogo José Fernandes Gonçalves

"Logic will get you from A to B.
Imagination will take you everywhere."

Albert Einstein

Contents

List of Figures

List of Tables

Abreviaturas e Símbolos

ADC	Application Delivery Controller
API	Application Programming Interface
BLE	Bluetooth Low Energy
DOF	Degrees of freedom
GATT	Generic Attribute Profile
IDE	Integrated Development Environment
IMU	Inertial measurement unit
I2C	Inter-integrated Circuit
MEMS	Microelectromechanical systems
MOEMS	Microoptoelectromechanical Systems
NEMS	Nanoelectromechanical Systems
SD	Serial Data
SoC	System on Chip
SPI	Serial Peripheral Interface
SS	Slave Select
RF	Radio Frequency
RF MEMS	Radio Frequency Microelectromechanical Systems
UART	Universal Asynchronous Receiver/Transmitter
USB	Universal Serial Bus
VO2	Oxygen Uptake
WBAN	Wireless body area network

Chapter 1

Introduction

1.1 Context and motivation

Since the invention of bicycles that cycling remains one of the major means of transportation all around the world. As a sport modality cycling has become extremely popular worldwide, either as a competitive or recreational activity.

In cycling the interaction between the body and the bicycle is a complex issue. The athlete's position is influenced by many different variables, including anthropometric measurements, athlete's strength and flexibility, muscle recruitment patterns and lower limb muscles lengths [Wishv-Roth, 2009]. The geometry of the cyclist-bicycle complex can influence the magnitude and direction of pedal force application, pedaling technique, physiological efficiency, probability of injury, aerodynamic friction and comfort in the bicycle [Welbergen and Clijsen, 1990] [De Vey Mestdagh, 1998] [Wishv-Roth, 2009] [Kleinpaul et al., 2010].

Several researchers recently reported that understanding the geometry and research around optimal configuration of the bicycle components is vital to maximize performance and minimize injury for both recreation and elite cyclists [Wishv-Roth, 2009][Bini et al., 2011] [Peveler et al., 2007].

Injuries are a common and unfortunate scenario that affects many cycling athletes and which may be associated with diverse factors. Overuse injuries occurs in most of the practitioners of this modality and can be a result of poor positioning of the athlete on the bicycle [Bini et al., 2011]. In cycling the knee joint is one of the most affected by overuse injuries [Wanich et al., 2007] [Asplund and St Pierre, 2004]. According to Bini et al. [2011] the occurrence of overuse knee joint pain in cyclists is about 50% . There are several causes of overuse injuries of the knee in cycling but the most common is improper configuration of the saddle height [Peveler et al., 2007]. When the saddle height is too low it can result in anterior knee pain, because it increases the knee angle and leads to increased compression of the knee and when the saddle height is too high it can result in posterior knee pain, due to the over extension of the knee at the bottom of the pedal stroke [Peveler et al., 2007] [Burke and Pruitt, 2003].

Numerous studies have shown that cyclists have to optimize their body positioning on the bicycle, which subsequently improve their pedaling movement in order to maximize factors of performance such as mechanical power production and muscular efficiency, and minimize the risk of overuse injuries associated with highly repetitive movements [Martin and Brown, 2009] [Silberman et al., 2005] [Bini et al., 2011].

Current techniques rely on bicycle fitting and laboratory measurements, which are based on camera analysis systems that use markers attached to the body of the athlete [Sauer et al., 2007]. Experiments have been conducted on laboratory environments to study the body kinematics during regular cycling, but these systems have as major drawback the inability of assess and monitor the kinematics of the cyclist in real life conditions, during training or competition [Fronczek-wojciechowska et al., 2016] [Marin-Perianu et al., 2013].

The use of auxiliary systems for the improvement of training methodologies and subsequently enhance the cycling technique and performance may be of extreme importance to the athletes and coaches in order to achieve the desired goals.

Recently miniaturized sensing systems, using micro-electromechanical systems (MEMS), came up to become a potential alternative solution to camera-based systems [Silva, 2014] [Mayagoitia et al., 2002] [Fong and Chan, 2010]. These systems need to be accurate enough to provide reliable measures and small enough to allow the use in outdoor context. The gold standard of these devices are the inertial measurement units (IMUs), which are composed by accelerometers, gyroscopes and magnetometers.

The monitoring of an individual's movement, not only applied to sport but also to health, has been an area of great study and development in the Wireless Body Area Network (WBAN) systems [Patel and Wang, 2010]. This type of system are composed by MEMS sensors for allowing a convenient and comfortable placement in the body of the patient or athlete, and in addition, given the applicability, also require efficient batteries, which together with the low consumption by the components can contribute to increase the autonomy and thus obtain a better performance of the system. The precision and accuracy of the acquired data are important challenges in this type of networks, due to their sensitive nature.

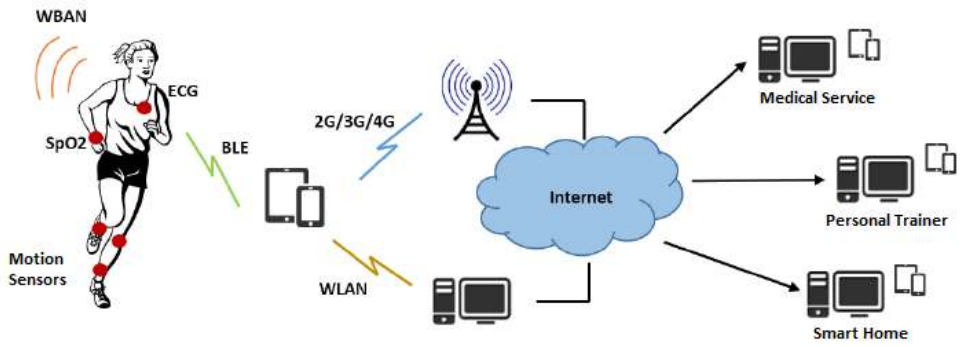

Figure 1.1: General scheme of interaction between components of a WBAN and other networks. adapted from [Maio, 2014]

In a WBAN (see figure 1.1), normally the data collected by the sensors is sent to a central station with the capacity to collect and perform the respective treatment. PCs started out as the ideal central station because they had great processing power and enough memory to handle and store the data collected. With the technological advance, smaller personal devices also began to assume the role of central station, as they had the advantage of presenting greater portability and continue with a good level of processing power. Nowadays smartphones have very advantageous characteristics for the use in monitoring system, since they present a high level of data processing, storage memory and compatibility with short distance communication protocols, such as Bluetooth Low Energy technology.

In high performance sports, the use of wireless body-area network systems based on wireless sensors, for collect valuable information in a real-time context is appealing to athletes and sport coaches. In the concrete case of cycling there are not many systems developed with this scope to evaluate and monitor the athlete's movement compared to other sports, such as swimming, running, among others. For all that has been refered can be concluded that there is a need in cycling for portable systems that can continuously monitor the kinematics of the cyclist, process the data to detect movement alterations and provide real-time feedback that can be used to improve the athlete's performance.

The Android operating system is currently the most used worldwide and being in constant development and growth, provides the programmer with a wide range of tools to be used in various applications in various areas. Therefore the introduction of the Android platform in this dissertation has allowed for greater flexibility and portability of the measurement system.

1.2 Aims and objetives

In a first stage the objectives were: analyze and understand the different variables that affect the performance in cycling, identify the most important and influential parameters which influence the performance of an athlete, elaborate the state of the art on the various measurement systems used by different researchers to evaluate and access cycling performance.

All this contribute to the final aim of this dissertation, the development and implementation of a system for measure the performance of human movement in sport activities, namely in cycling. This system, in addition to provide the athlete with parameters of interest for the improvement of training methodologies and consequently optimize the athlete's performance, should allow a real-time feedback for instant monitoring. In addition, the system should also store the data in an internal memory, allowing a more detailed analysis at the end of the training session.

In this way, for the implementation of the system the specific objectives are: 1. Hardware development; 2. Implementation and testing of data acquisition and storage algorithms; 3. Implementation of a wireless communication network between the device and the smartphone, via BLE; 4. Development of an Android Application; 5. Final testing to prove the concept.

1.3 Contributions

Often cycling experiments are conducted in laboratory environments to study the body kinematics during regular cycling, but these systems presents as major drawback the inability of assess and monitor the kinematics of the cyclist in real conditions, during a training session or in competition.

Thus, this study intends to allow to the athlete and coach to monitor in real time and in real conditions, permitting an improvement of training methodologies and consequent enhancement of the cycling technique, contributing to a better performance in the athlete under study.

1.4 Structure

This master thesis was organized in six chapters. Chapter 1 introduces the dissertation focus. Chapter 2 reports the state of art in the research of the optimal body positioning in cycling and his importance in the performance of the athlete as well as the systems developed by other researchers in this field. Chapter 3 introduces the technological background which will serve as basis for the development of the measurement system. Chapter 4 describes in detail the implementation of the monitoring system for cycling. It described all the hardware and software used in the development of the measurement system. In Chapter 5 the results are presented and discussed. Finally, Chapter 6 presents the conclusions and possible improvements.

Chapter 2

State of art

This chapter presents the state of art in the research about the optimal body positioning in cycling. Initially are reported the importance of achieving a proper position on the bicycle. Then is presented the methods for configuring saddle height adjustment and its importance in the performance of the athlete. Finally, the most relevant systems developed by other researchers for the evaluation of cycling based on inertial measurement units will be presented and described.

2.1 Body positioning on cycling

Scientific and empirical research has shown that the correct position on a bicycle is determined by several factors. The system that illustrates the correlation between them is formed by the following factors: friction, efficiency, maximization of pedaling power and comfort [Burke and Pruitt, 2003] [Kleinpaul et al., 2010]. However, many amateur cyclists, and even professionals, continue to adopt incorrect positions on their bicycles [Martins et al., 2007].

Burke and Pruitt [2003] stated that "for the cyclist interested in performance, to achieve a proper position on the bicycle is paramount". A properly fitted cyclist will be efficient, powerful, comfortable, and injury free on the bike. An efficient and powerful position is one that enables the cyclist to pedal the bicycle effectively, without a lot of wasted energy and improper pedaling mechanics [Burke and Pruitt, 2003].

In table 2.1 is presented a summary of experimental studies performed by several researchers, according to the type of adjustment used and the practice level of the subjects that conducted the experiments. This table shows the types of adjustments studied in the literature, general settings when considering the adjustments as a whole, and specific (saddle height or trunk positioning) when considering only one adjustment. Although different outcomes are measured between the studies, they all have a common goal, the search for optimum positioning of the cyclist.

In one of the studies on body position on cycling with greater richness in details of the description of the evaluations and variables considered for the good positioning of the cyclist, Martins et al. [2007] evaluated and compared the positioning on the bicycle adopted by 36 cyclists on their

Table 2.1: Summary of experimental studies examining body positioning on cycling

Reference	Adjustement	Subjects cycling level
Peveler and Green (2011)	Saddle height	Competitive
Bini et al (2011)	Saddle height	Recreational and competitive
Alencar e Matias (2009)	General settings	Recreational and competitive
Sanderson and Amoroso (2009)	Saddle height	Recreational
Peveler (2008)	Saddle height	Recreational and competitive
Diefenthaeler (2008)	Height and saddle advance	Competitive
Dorel (2007)	Trunk positioning	Competitive
Martins (2007)	General settings	Recreational and competitive
Peveler (2007)	Saddle height	Recreational and competitive
Sauer (2007)	General settings	Competitive
Peveler (2005)	Saddle height	Competitive
Silberman (2005)	General settings	Recreational and competitive
Ashe (2003)	Trunk positioning	Recreational
Burke and Pruit (2003)	General settings	Recreational and competitive
Savelberg (2003)	Trunk positioning	Recreational
Mestdagh (1998)	General settings	Recreational and competitive

own bicycles, nineteen of them competitive and seventeen recreational athletes. For the evaluations, a protocol was used as proposed by Burke and Pruitt [2003]. Positioning imbalances were detected in 82% of the recreational cyclists and 74% of the competitive cyclists' evaluated [Martins et al., 2007]. The most common errors related to the vertical and horizontal positions of the saddle, observed for 82% of recreational cyclists and 79% of competitive cyclists were found for seat adjustments. The second error with a large number of observations was relative to the height of the handlebar, observed in 12% of recreational cyclists and 5% of competitive cyclists [Martins et al., 2007]. Based on these results and as expected, recreational cyclists are more susceptible to misalignments in the body positioning than competitive cyclists.

De Vey Mestdagh [1998], Burke and Pruitt [2003], Silberman et al. [2005] and Alencar and Matias [2009] made a general survey of the adjustments to be adopted for saddle, handlebar, foot positioning on the pedal, and adequate size of the bicycle frame as well as other factors that may contribute to the good positioning of the cyclist. De Vey Mestdagh [1998] points out that adjustments can be based only on external anthropometric measurements of cyclists, while Silberman et al. [2005] also suggest the use of both static and dynamic adjustments. However, when it comes to elite cyclists, the cyclist-bicycle complex regulations must respect individual characteristics, because relatively small adjustments can exert a great influence on the performance of these athletes.

Burke and Pruitt [2003] reported that most cycling disciplines can fit into one of three classic body positions (figure 2.1). In figure 2.1a the cyclist adopts an upright trunk, almost vertical, with a slight backward saddle position, and represents the typical mountain-bike and recreational positioning. This position is not projected for aerodynamic benefit, but for a comfortable relaxed ride with improved vision, stability, traction, and handling characteristics [Dinsdale and Dinsdale,

2012]. Figure 2.1b represents the position adopted by road race cyclists, which provides to the athlete a compromise between speed, handling and comfort [Dinsdale and Dinsdale, 2012]. Figure 2.1c is the classic road time-trial and triathlon position. In this extreme aerodynamic position the athlete adopts a forward saddle position, with a highly flexed trunk, designed to minimize frontal area and aerodynamic drag, in the quest for speed [Dinsdale and Dinsdale, 2012].

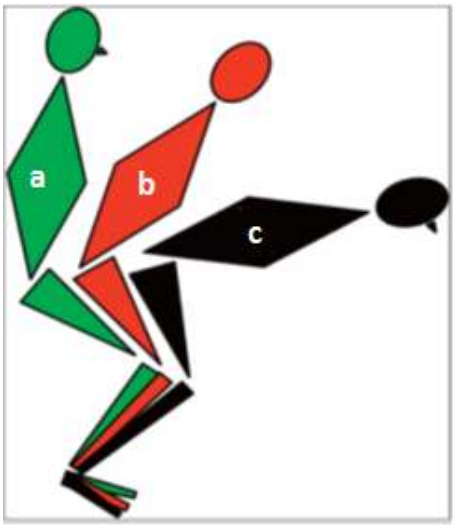

Figure 2.1: The 3 classic body positions in cycling [Burke and Pruitt, 2003].

The upper body positioning, and more concretely, the inclination of the trunk, is an important factor for altering the muscle recruitment and properties during pedaling [Savelberg et al., 2003] [Dorel et al., 2009] [Diefenthaeler et al., 2008]. This angle of inclination that characterizes many competitive postures still causes incorrect biomechanical postures that generate different patterns of support on the bicycle which can affect the cyclist performance [Dorel et al., 2009].

Savelberg et al. [2003] studied the effects of the position of the trunk of cyclists on the pattern of muscle recruitment. Changes in the position of the trunk, forward or backward, affected the ankle and hip kinematics, as well as thigh orientation. A similar pattern was found for muscle electrical activity. Both for the muscles that cross the hip joint and those that cross the ankle joint, there were changes in the activation period and the amplitude of the electromyographic signal.

Ashe et al. [2003] compared cardiovascular and respiratory variables of untrained cyclists, assuming two different positions when cycling, upright and aerodynamic position. In this study, ten physically active men, aged 17 to 25, underwent maximal exercise testing and steady state cycling at different workloads (50, 100 and 150 W). The results obtained at maximal effort shows that in the upright position, greater heart rate, oxygen consumption and maximum working load were observed in the participants [Ashe et al., 2003]. During steady state cycling, at the three workloads, oxygen uptake (VO2) and gross mechanical effort were greater in the upright position. Ashe et al. [2003] concluded that cyclists need to weight body position effects against the aerodynamic advantages of the aerodynamic position.

The most controversial aspect of bicycle configuration is saddle height and, consequently,

this has been the focus of most studies regarding body positioning on the bicycle [Sanderson and Amoroso, 2009] [Peveler, 2008] [Peveler et al., 2005] [Peveler et al., 2007]. Several researchers identified the saddle height adjustment as critical for optimal performance and injury prevention in cycling. The saddle height configuration can affect different factors which influences cycling performance, like energy expenditure, oxygen uptake, power output, cycling economy or pedal force application [Bini et al., 2011] [Faria et al., 2005].

2.2 Saddle height adjustment

Since initial investigations of saddle height on physiology and performance (Hamley and Thomas [1967]) sports scientists have been searching for the 'optimal' configuration of bicycle components to increase performance and prevent injuries [Peveler, 2008]. It is of primary importance for a cyclist to have saddle height properly adjusted to prevent injury and perform optimally. The methods for determining optimal saddle height are varied, and have been based on relationships between saddle height and lower limb lengths or a reference range of knee joint flexion [Bini et al., 2011].

2.2.1 Methods for configuring saddle height

In this topic will be reported the methods described in the literature for configuring saddle height. These can be divided into two groups, one based on percentage of lower leg length and the other based on a reference knee angle range.

2.2.1.1 Percentage of lower leg length methods

This methods are all based on anthropometric length measurements of the lower leg for configuration of saddle height.

Hamley and Thomas [1967] proposed probably the first research-based method for saddle height. In this method saddle height is determined by using 109% of inseam leg length (see figure 2.2), measured vertically from floor to ischium in the standing position [Hamley and Thomas, 1967].

The trochanteric leg length method (see figure 2.2) uses the length from the most prominent bony surface of the greater trochanter to the floor [Nordeen-Snyder, 1977] [Bini et al., 2011].

The length from the ischial tuberosity to the floor method (see figure 2.2) is determined with the cyclist standing and the distance taken between the most prominent bony surface of the ischial tuberosity to the floor [Shennum and DeVries, 1976] [Bini et al., 2011].

Other method proposed by saddle height configuration is the Greg LeMond method, which involves the measurement of the inseam leg length and the configuration of the saddle height based on 88.3% of the distance between the top of the saddle and the center of the bottom bracket [Burke, 2002]. It is important to note that this method does not consider differences in the crank

Figure 2.2: Examples of lower leg length measurements: (a) ischial tuberosity; (b) trochanteric length; and (c) inseam leg length. [Bini et al., 2011]

length dimensions [Bini et al., 2011]. Longer crank length results in lower pedaling cadence and smaller knee flexion angle [Macdermid and Edwards, 2010].

The empirical heel method (see figure 2.3a) is determined by when the cyclist is seated on the saddle, the knee must be fully extended when the heel is on the pedal and the crank is in line with the seat tube [Burke, 2002] [Bini et al., 2011].

2.2.1.2 Knee angle methods

This methods determines the saddle height according to a reference knee angle range. The Holmes method (see figure 2.3b) involves the measurement of flexion angle of the knee when the pedal is at the bottom dead center and the cyclist is seated on the saddle [Holmes et al., 1994]. In this method saddle height is determined by using a 25 to 35° knee angle.

Burke [2002] reported a variation of the Holmes method, as the Howard Method, for a knee angle of 30° with the pedal at the bottom dead center and the cyclist seated on the saddle. Similar to the Holmes method the knee angle measurement depends on the ankle angle, therefore, increasing ankle plantar flexion results in higher knee flexion angle [Bini et al., 2011].

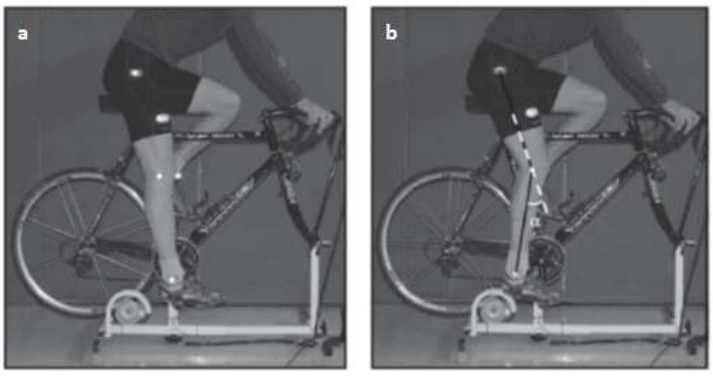

Figure 2.3: Saddle height configuration based on (a) the heel method; (b) the Holmes and the Howard methods. [Bini et al., 2011]

2.2.2 Effects of saddle adjustment in cycling performance

Formerly the cycling literature suggested that a 25 to 35° knee angle is most favorable for injury prevention, whereas a saddle height set using 109% of inseam is ideal for optimal performance [Hamley and Thomas, 1967] [Holmes et al., 1994] [Nordeen-Snyder, 1977] [Shennum and DeVries, 1976].

Since Hamley and Thomas [1967] reported that bicycle saddle height affected time to exhaustion during constant workload cycling trials, several studies have investigated the effects of saddle height on cycling performance parameters.

According to Price and Donne [1997] any relationship between maximal performance and saddle height depends on the optimization of pedal force application. The adjustment of saddle height subsequently affect the ankle angle [Peveler et al., 2007] [Ranklin and Neptune, 2008] [Diefenthaeler et al., 2006], which works as a link between the force produced in the hip and knee joints and the crank [Bini et al., 2011] [Mornieux et al., 2007].

Peveler et al. [2005] compared three methods of adjusting saddle height in the literature to verify which of them ensured that the knee flexion angle was between 25 and 35° when the pedal was in the bottom dead center. According to their experiments the leg length methods did not ensure the same knee joint angle range, and only 13 of 19 cyclists reached the desired knee angle range (25 to 35°) using either method [Peveler et al., 2005].

Peveler et al. [2007] performed anaerobic tests on trained and untrained cyclists with the purpose to determine if there is a difference on anaerobic power production between these two methods for saddle height configuration. Power output is also a strong predictor of performance in cycling [Faria et al., 2005] [Balmer et al., 2000] [Hamley and Noakes, 1992]. With their experiments, Peveler et al. [2007] proved that subjects riding with a saddle height set using the Holmes method could perform equally or greater than a saddle height set using the Hamley and Thomas method. According to the results obtained by Peveler et al. [2007] is suggested for both injury prevention and performance, the setting of saddle height using a knee angle between 25 and 35°.

Recent studies have established that saddle height based on inseam leg length is problematic as they tend to produce highly variable knee angles [Peveler et al., 2005] [Peveler et al., 2007], possibly due to anthropometric differences, femur, tibia, foot differences [Bini et al., 2011], or perhaps mechanical differences, variation in pedals, cleats, shoes and saddles [Dinsdale and Dinsdale, 2012]. Consensus of recent studies recommends an optimum saddle height for trained and untrained cyclists of 25-35° knee angle, for anaerobic power output [Peveler et al., 2007] [Peveler and Green, 2011], aerobic power output and cycling economy [Peveler, 2008] [Peveler and Green, 2011]. More specifically, Peveler and Green [2011] found VO2 was significantly lower at a saddle height of 25° knee angle compared with 35° knee angle.

Bini et al. [2011] and Alencar and Matias [2009] also suggests the setting of the saddle height with the knee flexion angle method (25 to 35°) to reduce the injury risk and to minimize the oxygen uptake by the athlete. One of the effects related to an improper saddle height configuration is that more oxygen becomes consumed by the athlete, which means a loss in his cycling efficiency.

In summary, a saddle height set to a knee flexion angle 25-35° is desirable for reducing knee injuries and improving performance in trained and untrained cyclists.

2.3 IMU's applications on cycling

Miniaturized sensing systems have become potential alternative solutions to the camera systems. Inertial and magnetic sensors such as accelerometers, gyroscopes and magnetometers have recently been introduced as alternatives in the evaluation and monitoring of cycling. In the last decade researchers in this area have shown great interest in this field due to improvements in the accuracy, size and cost of MEMS systems.

In recent years many researchers have developed studies on kinematic analysis in various sports using IMUs. In sporting activities such as running (Bergamini et al. [2012]), jumping (Picerno et al. [2011]) or swimming (Peiwei [2012]) these devices have been widely accepted. However, in cycling analysis they still very limited.

The sampling frequency is also a very important feature when the goal is to detect human movement. According to Zhou et al. [2009], when the sampling frequency is twice as high as the frequency of human movement, it is possible to detect this through sensors. However, a high sampling frequency requires more time and processing power, which is not advisable on IMU devices. Zhou et al. [2009] after analyzing several sampling frequencies, stated that a frequency of 40 Hz is sufficient for the recognition of human movement. For this frequency, it obtained an accuracy of 93 % and a processing time of 0.253 seconds to distinguish seven gestures. In previous research made by Bouten et al. [1997] and Sun and Hill [1993], the authors stated that the lowest sampling frequency to achieve an acceptable monitoring of human activities is 20 Hz.

Next, it will be described two examples of measurement systems developed to evaluate and monitor the athlete's behavior during cycling activity, both of them based on inertial measurement units.

2.3.1 Systems description

Maio [2014] developed a measurement system for monitoring the cycling posture. This system measure the tilt angle of the trunk of the athlete, the tilt angle of the bike and the knee angle of the athlete. The positional data are obtained through the IMU's presented in the sensory nodes and then sent (through BLE) for a smartphone, which plays the role of central station.

In this prototype for posture monitoring applied to the evaluation of cyclists, 3 sensory nodes are distributed throughout the athlete's body: one in the chest, in order to measure the inclination of the torso relative to the bicycle, one in the upper leg (thigh) and the third one in the lower leg (shank), in order to obtain the angle formed by both segments [Maio, 2014].

Each sensory node consists of a set of 3 sensors, accelerometer, magnetometer and gyroscope, which capture the variations on each of its 3 axis (resulting in 9 degrees of fredoom). The data collected by the sensory nodes are then sent via BLE to an android application.

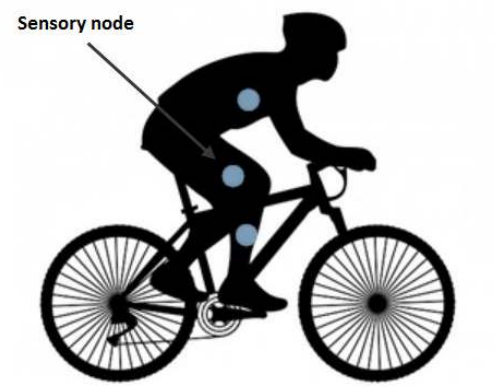

Figure 2.4: Sensory nodes placement of the developed system for posture monitoring by Maio [2014].

In order to measure the inclination of the bicycle (necessary for the calculation of the inclination of the trunk), Maio [2014] used the sensors of the smartphone, which is placed on the handlebar of the bicycle, being an ideal position for this measurement, instead of placing another module on the bike, taking advantage of the sensor system of the smartphone and thus taking more advantage of the equipment.

The developed application called "Cycling Kinect", aims to monitor the cycling athlete's posture during a training race or competition. The application is executed on the smartphone, which assumes the role of central station and serves as interface with the user, in this case, the athlete [Maio, 2014]. The application receives periodically the information collected by sensory nodes, present in the body of the athlete, and with these data, after appropriate treatment, calculates his posture [Maio, 2014].

It is important to mention that the sensory nodes used by the researcher for the implementation of this system had already been developed, and his research was mainly focused on the data communication and its efficiency.

Other approach was presented by Marin-Perianu et al. [2013] with the design of a portable wireless sensor network for real-time monitoring of lower limb kinematics during cycling. Due to the importance of the joint kinematics to assess the cycling technique and subsequently the cycling performance, this system focus on the measurement of knee and ankle angles.

In their research Marin-Perianu et al. [2013] besides the measurement system for monitoring cycling kinematics introduce as well an algorithm for computing the orientation angles that propose an innovative way of fusing the data from the accelerometer, gyroscope and compass sensor. The algorithm exploit the cyclic nature of the motion and introduce a reset step for avoiding the accumulation of integration errors, instead of the use of traditional filtering techniques [Marin-Perianu et al., 2013].

The sensing system is composed by several area wireless inertial sensor nodes based on the

ProMove platform. Each node has an inertial measurement unit with 8 degrees of freedom, three-axial accelerometer, three-axial magnetometer and a two-axial gyroscope.

The system proposed by Marin-Perianu et al. [2013], is composed by three ProMove nodes placed on the thigh, shank and foot of the cyclist (see figure 2.5). This system compute for each node its orientation relative to the Earth reference frame in terms of roll, pitch and yaw angles. Through the combination of the orientation of each node, is possible to obtain the joint motions of the three segments of the lower limb [Marin-Perianu et al., 2013]. The knee and ankle angles were computed using the roll angles derived from the motion of the three nodes in sagittal plane.

Figure 2.5: ProMove nodes placed in thigh, shank and foot of the subject [Marin-Perianu et al., 2013].

In the study performed by Marin-Perianu et al. [2013] was used a reference motion analysis system in order to validate the performance of the developed measurement system. The reference camera-based system used for comparative purposes was Optotrack Certus, Northern Digital Inc.

For their experiments, Marin-Perianu et al. [2013] mounted both systems on the athletes. The Optotrack system is composed by infra-red markers that were placed at the anterior surface of mid-thigh and mid-shank and at the superior surface of the foot, and then were tracked while subjects were pedaling [Marin-Perianu et al., 2013]. Nine professional and recreational cyclists performed the tests with their own bikes positioned on roller cylinders.

For a better comparison between the data collected by sensor nodes and the camera system, Marin-Perianu et al. [2013] defined the sampling frequency at 200Hz for the two systems. Before each experiment both the sensor nodes and the camera system were calibrated.

The raw data collected from sensor nodes was processed on the computer using Matlab software, in order to compute the angles of knee and ankle joints [Marin-Perianu et al., 2013]. At the beginning of each experimental session, the accelerometer and magnetometer are used to establish the orientation of each node (roll, pitch and yaw angles). During cycling, the gyroscope and magnetometer are used to measure the variation of the roll angle and subsequently compute the joint angles [Marin-Perianu et al., 2013].

Despite concluding that both systems are highly correlated, the wireless system has several advantages such as flexibility due to the absence of cables, ease of usage in outdoor environments and the ability to perform algorithms, which guarantee high precision in measurements, in low energy microprocessors [Marin-Perianu et al., 2013].

The authors present the ideal solution for their system using a smartphone or tablet that would serve as a central station to receive and process data in order to provide the athlete with real-time feedback, but at the time of publication of their study this part of the system was not yet implemented, and the data were processed in Matlab to obtain knee and ankle angles.

2.3.2 Overall considerations

The systems presented above will serve as a reference for the development and implementation of the measurement and monitoring system for cycling.

In Table 2.2 is presented the general characteristics of this two systems.

Table 2.2: General characteristics of the two systems

Reference	**nº modules**	**location**	**IMU's**	**Outcome measures**
Maio, 2014	3 + smartphone	thigh shank trunk	3 axis accelerometer 3 axis gyroscope 3 axis magnetometer	knee angle trunk and bike inclination angle
Perianu, 2013	3	thigh shank foot	3 axis accelerometer 2 axis gyroscope 3 axis magnetometer	knee angle ankle angle

Both investigators have identified the calculation and monitoring of knee angle as a primary factor, since as previously mentioned, this angle should be in the interval of 25° to 35° for a performance optimization and reduction of the athlete's injury risk.

The monitoring of the ankle joint is also an important factor for the athlete's performance, but this angle is a consequence of the knee angle, so with a knee flexion angle in a range of 25 to 35° the athlete's ankle joint will be in a good angle interval. The monitoring of knee and ankle joints it is of extreme importance for the athlete because these joints have direct influence on the power transmitted to the pedals.

Chapter 3

Technological Background

This chapter presents the technological background that will serve as basis to the development of the measurement system for evaluation of cycling performance. First, the operating principles of the MEMS inertial sensors are described. Next, is introduced all the concepts related to BLE communication technology and is presented a comparison to other similar technologies. Finally is presented an overview on the two communication protocols used in communication between the various modules of the physical device, namely SPI and I2C.

3.1 MEMS-based inertial sensors

Micro-Electro-Mechanical-Systems (MEMS) can be defined as "mechanical devices that have a characteristic in length of less than 1 mm but more than 1 μm, combining electric and mechanical components" [Maluf and Williams, 2004]. This microsystems integrates mechanical and electrical elements to perform certain functions, and they were incorporated into our day-to-day life as sensors, actuators, electronic components and micro-structures [Maluf and Williams, 2004].

Due to different components and applications, MEMS have different designations to describe, such as RF MEMS (radio-frequency MEMS) for radio- frequency applications, MOEMS (micro-optoelectromechanical systems) for optical devices, NEMS (nanoelectromechanical systems) in nanoscales and bioMEMS for bio-related applications [Ma, 2015].

Currently MEMS technology is employed in the manufacture of various types of commercially available sensors, namely the inertial sensors. MEMS inertial sensors have many advantages when compared to conventional sensors in terms of weight, impact resistance, energy consumption and, especially, the reduced cost of production. The manufacturing processes of these sensors are similar to those used by the microelectronic components industry (integrated circuits), facilitating large-scale production [Romig et al., 2003].

The development of miniaturized low-power accelerometers and gyroscopes allowed the successful application of these systems in cost-sensitive areas, from rehabilitation to sports, entertainment and automotive industries.

Recently inertial sensors have been increasingly used to monitor human movement, biomechanics and relate this data to the tasks associated with every-day living and sports activities [Espinosa et al., 2015]. These sensors have been successfully utilised in different sports related to monitoring research projects [Setuain et al., 2015] [Khurelbaatar et al., 2015].

3.1.1 Inertial sensors principles

According to Tamura [2014] "the coordinate system must be defined prior to deployment of an inertial sensor for body motion measurement". If the origin of a moving coordinate system has acceleration (Ao) and rotates with a gyroscopic angular velocity (ω), and if a mass (m) has the position vector (r') and the velocity (u') with respect to the moving coordinate system, then the inertial force observed is:

$$mA' = -mAo + 2mu' \times \omega + m\omega \times (r' \times \omega) + mr' \times \frac{d\omega}{dt} \tag{3.1}$$

where ' indicates a variable corresponding to the moving coordinate system. The four terms on right side of the equation results from the angular accelerations that correspond to the linear inertial, Coriolis, centrifugal, and apparent forces [Tamura, 2014].

3.1.2 MEMS accelerometers

MEMS accelerometers have become an attractive tool for use in wearable systems for detecting and measuring aspects of human movement [Silva, 2014].

The purpose of accelerometers is to measure linear accelerations in a very precise way. These signals are typically expressed in m/s^2 or are related to the constant gravitational acceleration g.

Typically the accelerometer has a movable mass which is connected to a fixed frame via spring structures (see Figure 3.1). When an external acceleration is applied to the mass, it will move relative to its initial position.

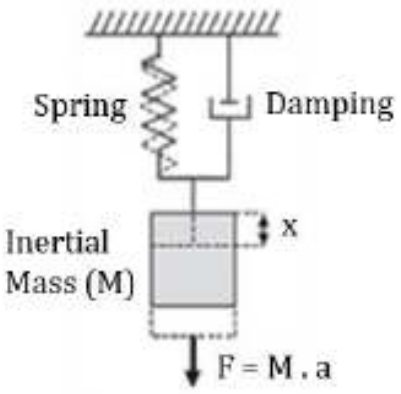

Figure 3.1: Accelerometer model [Silva, 2014].

The magnitude of the mass displacement is proportional to the magnitude of the acceleration and inversely proportional to the stiffness of the spring structures [Silva, 2014].

Determining the amplitude and direction of acceleration in three-dimensional space requires a triaxial accelerometer, as shown in Figure 3.2:

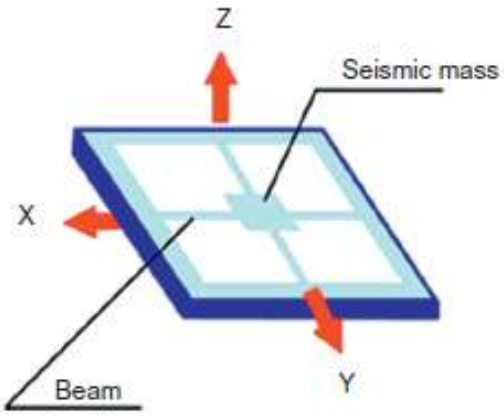

Figure 3.2: Tri-axial accelerometer Tamura [2014].

The conversion of the displacement of the proof mass into an eletrical signal can be fulfilled by different methods, includining those based on capacitance, piezoresistive or piezoelectric effects [Maluf and Williams, 2004].

Capacitive-based accelerometers are using the fact that the capacitance of a given plate capacitor is inversely proportional to the distance between the plates. If this distance changes due to a movement of the proof mass, the capacitance changes and the change in the electrical potential between the electrodes can be measured. In order to increase the sensor's sensitivity and to reduce the noise, many capacitors can be combined linearly to create the output signal [Nikolic et al., 2013].

Measuring capacitance alterations caused by displacement provides a large output signal, good steady-state response, and better sensitivity due to low noise performance. The capacitive sensors have as disavantadge the fact that they are suscetible to eletromagnetic fields [Silva, 2014].

The piezoelectric accelerometers have in their constitution synthetic or natural crystals that generate electric current when they are subjected a mechanical deformation [Nikolic et al., 2013]. On the other hand, applying an electric field on the crystals, generates a deformation. This effect is due to the physical disposition of the atoms in piezoelectric crystals.

In this type of sensors, the mass is attached to a piezoelectric crystal. When the accelerometer body is subjected to vibration, the mass obeys the laws of inertia and the crystals are subjected to forces of compression and / or traction, generating electric charges. According to Newton's second law (equation 3.2), these forces are proportional to acceleration.

$$F = ma \tag{3.2}$$

The sensitivity of these sensors is directly related to the piezoelectric coefficients that are different for each material and for each direction and therefore it is important to have a uniform crystal with the minimum of impurities. The piezoelectric crystal and the proof mass can be disposed in many different configurations, depending on the target application of the accelerometer [Nikolic et al., 2013].

Piezoresistive accelerometers are similar to piezoelectric ones, except that a change in mechanical stress F results in a change of the material resistivity. The resulting resistivity is also linear with the applied force for a given direction and material, and can be obtained by measuring the eletctric voltage U for a constante electric current I and using Ohm's Law :

$$U = R(F) \times I \tag{3.3}$$

Piezoresistive and piezoelectric-based accelerometers normally have a higher robustness and range than capacitive-based accelerometers but have less accuracy. According to Tamura [2014] due to these characteristics described above these accelerometers are the most used in the measurement of human movement. MEMS accelerometers have been becoming a very attractive tool in the development of wearable systems for the detection and measurement of parameters in human movement.

3.1.3 MEMS gyroscopes

A gyroscope consists in a spinning wheel mounted on a movable frame which can measure angular velocity. When the wheel is spinning, it tends to retain its initial orientation in space, regardless of the central forces applied to it [Tamura, 2014]. When the direction of the axis is externally altered, a torque proportional to the rotation rate of the axis of inclination arises, which can be used to detect angular velocity.

The principle underlying the operation of MEMS gyroscopes is the Coriolis Effect, which is a phenomenon observed when an object is moving with a certain velocity in a rotating frame of reference [Nikolic et al., 2013]. This effect establishes that an object with a velocity V and an angular velocity W about an axis perpendicular to the vector V is subjected to a Coriolis acceleration:

$$a_{cor} = 2\Omega \times V \tag{3.4}$$

The Coriolis force is proportional to the rotation speed of the frame of reference. Its direction is perpendicular to the rotation direction of the reference frame and to the velocity of the moving object [Nikolic et al., 2013].

$$\vec{F}_{Coriolis} = 2m_{object}\left(\vec{v} \times \vec{\Omega}\right) \tag{3.5}$$

By measuring the effect of this force on a proof mass which is moving at a known speed, the angular velocity of the frame of reference, this is, the object where the sensor is placed on, can be determined.

Currently, MEMS gyroscopes have a resolution of 0.01–0.1 degs $^{-1}$ Hz$^{-1/2}$. A major drawback of MEMS gyros is zero-point stability. This is due to the difficulty in measurement of the small displacement generated by Coriolis force, which often reaches hundreds of deg/s [Maenaka, 2008].

An example of a resonant structure used for MEMS gyroscopes is what is called a tuning fork, which consists in the combination of two beams of same length and material on a common shaft, which is excited at their resonance frequency, resulting in a type of balanced oscillator where the two beams oscillate 180 out-of-phase [Nikolic et al., 2013]. This structure is more energy efficient and more accurate when comparing with one beam. When a rotation of the system occurs in a direction perpendicular to the vibration direction of the beams, the resulting Coriolis force changes the frequency of the vibration, which can be detected using a piezoelectric or piezoresistive material [Nikolic et al., 2013].

Other vibrating structure used for MEMS gyroscopes is a vibrating plate, with circular or rectangular shape. The plate is suspended by spring structures such and an actuator makes this structure vibrate at a specific frequency and phase [Nikolic et al., 2013]. This vibration can be in an in-phase direction (x axis), in which case a rotation normal to the plane (z axis) causes the deviate to vibrate in the other in-plane direction (y axis). In figure 3.3 is shown two examples of this vibrating plate gyroscopes.

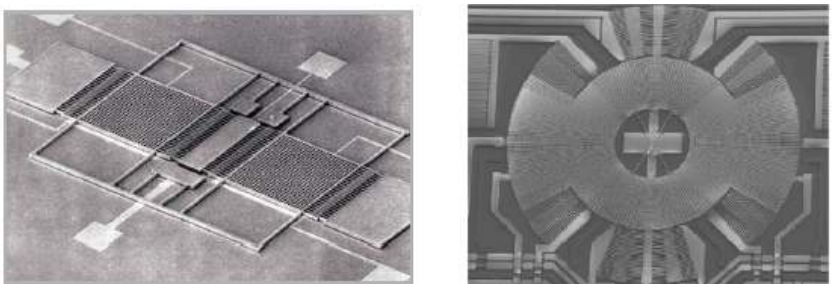

Figure 3.3: Examples of vibrating plate gyroscopes. [Nikolic et al., 2013].

3.1.4 Inertial Measurement Unit

Inertial measurements unit (IMU) sensors emerged in 1930s where because of its constraints in size, cost and power consumption were mainly used for aircraft navigation and in large size devices [Zhao and Wang, 2012].

Recently, the micro-electromechanical (MEMS) technology allowed the fabrication of IMU sensors with very small size, small cost and with low processing power, which result in a exponentially grow in the application areas of this sensors [Tanenhaus et al., 2012].

IMU sensors has been widely used to determine and assess human movements in terms of acceleration, angular velocity and rotation [Zhu and Zhou, 2004].

3.1.4.1 IMU technologies

The earlier technology of IMUs consists in a combination of two types of sensors, accelerometers and gyroscopes. The accelerometer is used to measure the linear acceleration while gyroscopes measure the angular velocity.

In this type of IMU each sensor have typically three DOF (degrees of freedom) defined for x, y and z axis which combining both sensors perform a total of 6 DOF. The readings obtained by the two sensors are kept separately. Angles can be measured from both sensors, thus both data can be calibrated as shown in figure 3.4 to obtain more accurate output data [Ahmad et al., 2013].

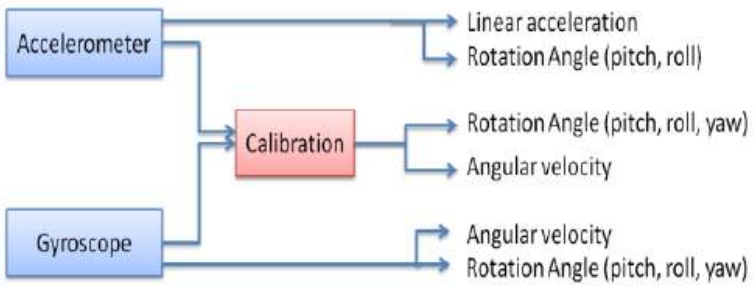

Figure 3.4: IMU based in two sensors [Ahmad et al., 2013].

The benefit of using this type of IMU is that it will not be affected by the external magnetic field when it is used close to ferromagnetic material. In contrast, as a drawback the measurements might not be accurate due to the sensors' noise and the gyroscope drift issue.

Later, another sensor came up to complement IMU technology, the magnetometer. This magnetic sensor measures the bearing magnetic direction, which consequently improve the gyroscope readings. Commonly the three sensors (accelerometer, gyroscope and magnetometer) that composes this IMU, get three axial measurements each, making the total of 9 DOF (figure 3.5). The magnetometer is used to measure yaw angle rotation, and it can used to calibrate the gyroscope data in order to improve the drift errors [Ahmad et al., 2013].

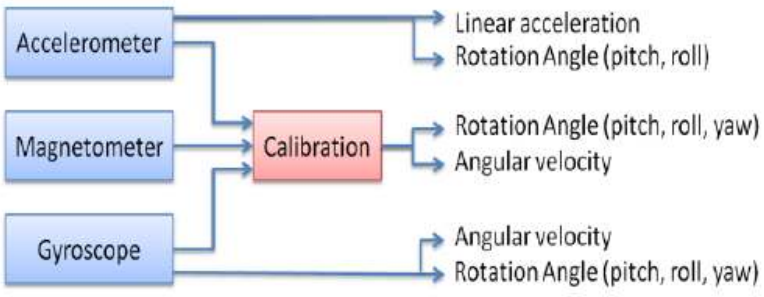

Figure 3.5: IMU based in three sensors [Ahmad et al., 2013].

This type of IMU is more accurate than the previous one because less drift errors occurs. The disadvantage of combining the magnetometer in this sensor is that if it is used in an environment surrounded by ferromagnetic material, the IMU measurements may be affected due to the disturbance to magnetic field [Zhu and Zhou, 2004].

Generally the higher the number of degrees of freedom, the more certain we can accurately sample the data [Ahmad et al., 2013].

3.2 Bluetooth Low Energy

Bluetooth wireless technology consists of a short-range communication system designed to replace the cables connecting the various fixed and mobile devices. Nowadays, the application's areas of this technology has increased considerably, having a strong impact in the areas of industry, multimedia, health and sport. Particularly in the areas of sports and health, bluetooth technology has been used in personal monitoring devices where portability is a key aspect.

Over the years, several versions of this technology have been released. Recently emerged the Bluetooth Low Energy (BLE) technology that was introduced as a controller of version 4.0 of the classic Bluetooth. The BLE system was developed with the purpose of transmitting very small information packets at a time, while at the same time presenting a very low power consumption when compared to systems that support controllers BR(Basic Rate)/EDR(Enhanced Data Rate), as the case of classic Bluetooth. This version was created to respond to the need to reduce energy consumption by this technology, increasing the durability of the devices in which it is used.

3.2.1 Architecture

The architecture of this technology is represented by a protocol stack divided into two main sections, which are the Controller and the Host, as we can see in the figure 3.6. The applications or profiles used are at the top of the protocol stack.

Beginning at the bottom of the BLE protocol stack, the physical layer operates in the 2.4GHz frequency band and defines 40 channels of radio frequency. There are two types of radio frequency channels in the BLE: advertising channels and data channels. There are three advertising channels which are used for advertisements related activities, device discovery, broadcast and connection establishment, while the remaining 37 data channels are used for bidirectional communication between connected devices [Gomez et al., 2012].

In BLE, there exists an 'advertiser' that transmits advertising packets at precise time intervals, and a 'scanner' that acts to receive data using the advertising channels [Touati et al., 2013]. In order to initiate the communication between BLE devices it is necessary a prior connection to begin a reliable bidirectional data communication. This communication is an asymmetric procedure in which the advertiser transmits advertisements packets through the respective channels, while the other device (scanner) that is the initiator listens these packets [Touati et al., 2013]. After receiving those packets the initiator transmits a connection request message to the advertising device which enables the connection establishment.

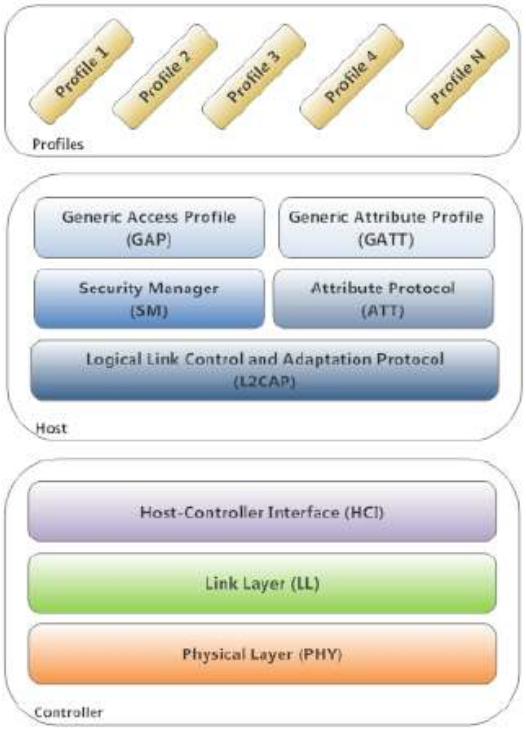

Figure 3.6: BLE Protocol Stack Maio [2014].

The Link Layer defines the devices as master and slaves, where the first ones initiate the connection (initiator) and the second ones announce their availability and accept the links (advertisers), during a connection establishment. The master can connect to several slaves. The slaves, in their basic routine operation, get into sleep mode and turn active periodically, to listen to the packets from the master [Touati et al., 2013]. Usually it is the master who defines the sleep and wake-up periods of the slaves.

The layer Host Controller Interface (HCI) provides the means of communication between the Controller section and the Host section through standardized interfaces. This layer can be implemented either through an API or through hardware interfaces such as UART, SPI or USB [Maio, 2014].

The Host section is divided in five sublayers. The Logical Link Control and Adaptation Protocol (L2CAP) manages the encapsulation of data to the upper layers, allowing a logical data communication between devices. This process is done in a best-effort approach without using retransmission mechanisms and flow control, unlike in other versions of Bluetooth [Gomez et al., 2012]. The upper layer protocols provide data structures that fit the maximum L2CAP payload size, which is 23 bytes [Touati et al., 2013].

The security manager layer defines the methods for pairing and distributes the security keys. This layer allows the other layers of the protocol stack to securely connect and exchange data with other devices. The data is read or written only when the connection is authenticated, and when it is formed, the two devices undergo a pairing process. When this process occurs, the keys are

established either to encrypt or to authenticate the connection [Instruments, 2015].

The Attribute Protocol (ATT) allows the expose of certain components of their data, called attributes, to other devices. Attributes are data structures that store information provided by the Generic Attribute Profile (GATT) layer. According to this protocol, a device that exposes its attributes is referred to as the server and the neighbor device is the client. The master/slave roles assigned in the link layer are independent of the client/server roles defined in this protocol [Gomez et al., 2012].

The GATT layer defines a framework for using the procedures from the ATT layer for service discovery and specifies the structure of the profiles [Gomez et al., 2012]. This layer contains the necessary procedures for communicating data between devices on a BLE connection. In this type of communication, it is called characteristics, all the data that is being used for a certain service. In a hierarchical way we can say that a profile can have several services and each service can have several characteristics. The definition of services and characteristics is organized in the form of attributes.

At the highest level of the BLE protocol stack is the Generic Access Profile (GAP) layer. This layer is the direct interface with the applications and/or profiles, being also responsible for the specification of device roles, modes and procedures for the discovery of devices and services, the management of connection establishment, and finally, for their security Touati et al. [2013]. This layer always operates in one of these four roles: broadcaster, observer, peripheral or central.

A device in the broadcaster role only transmits data through the advertising channels and does not support connections with other devices. The observer role works as a complement for the Broadcaster, this is, has the purpose of receiving the data transmitted by the broadcaster. The central device looks for the advertisements and initiates the communication, operating as master and can manage several connections, while the peripheral device is the annunciator that has the ability to connect and operates as a slave in a simple connection [Gomez et al., 2012].

3.2.2 Comparison with other technologies

Patel and Wang [2010] reviewed the several candidate wireless technologies which have favorable characteristics for use in wearable monitoring systems, as shown in table 3.1.

With the emergence of BLE technology, several comparative studies have emerged to evaluate the performance of BLE-based monitoring systems compared to other technologies. In their study Gomez et al. [2012] evaluated several parameters such as debit, latency, piconet size and energy consumption of BLE technology.

As already mentioned, energy consumption is a major concern when designing a monitoring device. The BLE technology has emerged to meet this need, as well as ZigBee technology. In Siekkinen et al. [2012] the researchers present an in-depth study comparing these two technologies. With regard to energy consumption, in fact, the BLE consumes extremely little energy, presenting a very attractive ratio of energy per bit transmitted.

Comparing classic Bluetooth with BLE technology implies that they have different contexts of use. Classic Bluetooth is applied when large amounts of information need to be transmitted,

Table 3.1: Characteristics of the various technologies used in wearable monitoring systems(Patel and Wang [2010]).

Technology	Spectrum	Channels	Data rate	Peak power	Consumption	Topology
Bluetooth	2,4 GHz	79	1-3 Mb/s	∼45mA/ 3,3 V	50 (nJ/b)	Scatternet
BLE	2,4 GHz	3	1 Mb/s	∼28mA/ 3,3 V	92 (nJ/b)	Piconet Star
ZigBee	2,4 GHz	16	250 Kb/s	∼16,5mA/ 1,8 V	119 (nJ/b)	Star, Mesh
ANT	2,4 GHz	125	1 Mb/s	∼22mA/ 3,3 V	73 (nJ/b)	Star, Tree or Mesh
Sensium	868 MHz 915 MHz	16	50 Kb/s	∼3mA/ 1,2 V	72 (nJ/b)	Star
Zarlink	402-405 MHz 433-434 MHz	10	200-800 Kb/s	∼5mA/ 3,3 V	21 (nJ/b)	P2P

whereas BLE has advantages when it is necessary to receive/send small data quantities periodically. Devices using classic Bluetooth have a much shorter battery life compared to devices that use BLE.

In conclusion, it can be said that BLE technology is best suited for sports and health monitoring applications, where easy portability and low consumption are essential factors for the good performance of the system.

3.3 Communication Protocols

Nowadays, is possible to find at the low end of the communication protocols the serial peripheral interface (SPI) and the inter-integrated circuit (I2C) protocols. Both protocols are well-suited for communications between integrated circuits, allowing the interconnection between devices and the exchange of information with each other [Leens, 2009]. I2C and SPI protocols coexist in many modern digital electronics systems, as both are actually quite complementary for this kind of communication [Leens, 2009].

In this section it will only be presented the I2C and SPI protocols, as they are the most indicated for the implementation of the measurement system.

3.3.1 I2C

The inter-integrated circuit protocol was developed in the 1980s by Philips and arises from the need to maximize hardware efficiency and circuit simplicity [Myers, 2007]. The I2C bus aims to facilitate communication between integrated circuits that were on the same printed circuit board.

The I2C bus is a synchronous, low-speed serial communication that is indicated for short distances. This is a multi-master protocol that always use two signal lines, in addition to the

common ground reference. These signals are serial data (SDA), responsible for data transportation, and clock signal (SCL), responsible for synchronization [Leens, 2009].

In this protocol, through the use of only two wires is possible to connect multiple devices allowing communication between them. A particular device can function as master or as slave. This protocol supports several masters and several slaves connected to the same bus, however only one master can operate at a time [Lynch et al., 2016a]. The master is responsible for the clock signal, defining the speed at which data flows. In the case that two or more masters attempts to control the bus at the same time, occurs an arbitration process that ensures that all but one of them drop out [Wilmshurst and Toulson, 2016].

I2C devices can operate in some specifics data rates, 100kHz, 400KHz and 3.4MHz, respectively called standard mode, fast mode and high-speed mode [Leens, 2009].

In figure 3.7 we can see the typical circuit of an I2C bus, in which several slaves are connected to the SCL and SDA lines of the same master device.

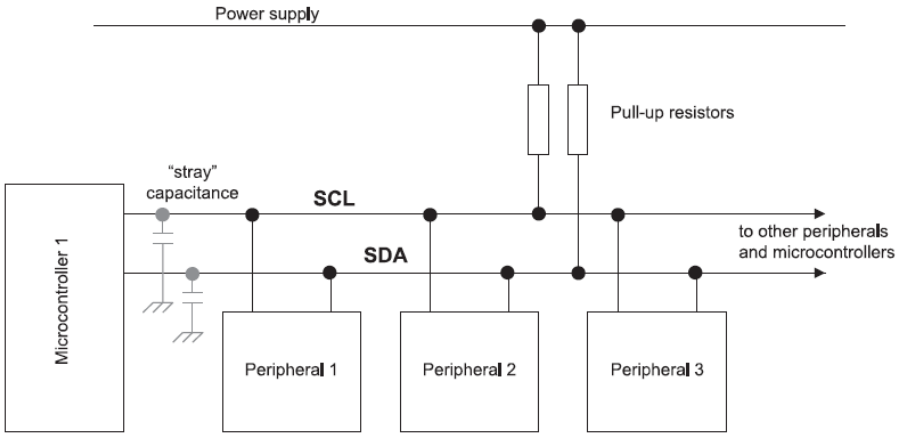

Figure 3.7: Example of an I2C bus configuration [Wilmshurst and Toulson, 2016].

3.3.1.1 Operation Mode

Data transfers follow the format shown in Figure 3.8. In order to begin a certain data transfer, the master generates the START condition (S) on the bus. This condition occurs when the SDA line moves from a high logic level to the low logic level, while the SCL line remains high [Leens, 2009] [Wilmshurst and Toulson, 2016] [Lynch et al., 2016a]. It then transmits the address consisting of 7 bits, which indicates the slave with which to communicate and an 8th bit that indicates the type of communication (R/W) - a 'zero' indicates a transmission (WRITE), a 'one' indicates a request for data (READ). If the slave is active at the address sent, it sends an acknowledgment signal (one bit) to the master initiating the transition. A data transfer is always terminated by a STOP condition (P) generated by the master, which corresponds to a transition from low to high level of SDA line while SCL line remains high [Leens, 2009] [Lynch et al., 2016a] [Wilmshurst and Toulson, 2016]. However, if a master still wishes to communicate on the bus, it can generate a repeated START condition and address another slave without first generating a STOP conditios [Phillips

Semicondutors, 2000]. Several combinations of read/write formats are then possible within such a data transfer.

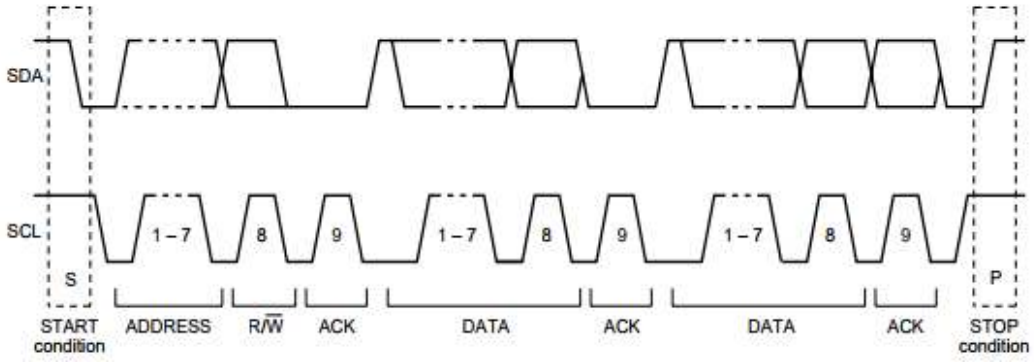

Figure 3.8: I2C complete data transfer [Phillips Semicondutors, 2000].

The number of bytes that can be transmitted per transfer is unrestricted, however, every byte put on the SDA line must be 8-bits long [Phillips Semicondutors, 2000]. As seen in the figure 3.8 each byte transmitted has to be followed by an acknowledge bit.

3.3.1.2 Advantages and Disadvantages

The main advantage of the I2C protocol is that it requires only two pins of the master device, regardless of the number of slaves used, that can go up to a maximum of 112 slaves when the identification address consists of 7-bit (2^7 = 128 combinations, but 16 of these are reserved addresses, which results in 112 available). Another advantage of this protocol is its simplicity and relative ease of implementation at the software level.

A disadvantage is the fact of operating at low speeds and therefore it is ineffective to use them in sensors that produce a lot of data in a given time interval. It is widely used in inertial, environmental (light and pressure) and proximity sensors, in which the data transmission rate is relatively low, compared to other sensors.

The I2C protocol dictates that clock and data lines must be at a high logical level when they are not in use, which is ensured by the pull-up resistors. This results in an inverse proportionality between speed and power consumption. Low resistances will increase the transmission speed, but the energy consumption will increase and the same happens inversely [Lynch et al., 2016a].

3.3.2 SPI

The Serial Peripheral Interface (SPI) protocol was introduced in 1979, with the first microcontroller deriving from the same architecture as the popular Motorola 68000 microprocessor [Leens, 2009]. Originally it had as purpose the communication between peripherals and the computer, but Universal Serial Bus (USB) technology has replaced SPI on those areas of application. However, it continued to be widely used in communication between chips and integrated circuits, being an

important method of communication in digital systems. This protocol has had a large influence in the embedded world [Wilmshurst and Toulson, 2016].

SPI is a synchronous, full-duplex serial communication, can receive and send data at the same time, which uses four lines for communication, two control lines and two data lines.

1. A clock signal (SCLK) generated by the master and sent to all the slaves.
2. A slave select signal (SS) used to select the slave which the master communicates with.
3. A data line named Master Input Slave Output (MISO), data goes from the master to the slaves.
4. A data line named Master Output Slave Input (MOSI), data goes from the slaves to the master.

SPI devices communicate using a master-slave relationship, in which the master initiates the data transfer. In this protocol there are only one master device and may be one or several slave devices. When the master generates the clock signal and selects a slave device, data can be transferred in either directions simultaneously. The two typical SPI bus configurations are shown in figure 3.9.

In the case of multiple devices connected, the master uses the SS line to select the slave with which pretends to communicate. The addiction of slaves to the system presupposes the addiction of new lines. Thus, if n slaves are connected to the master, n SS pins will be required. On the other hand, if the system is composed by only one slave this line is optional.

The SCLK, MISO and MOSI lines are shared among all devices, master and slaves. So in a configuration where n slaves are connected to the master will be needed (3 + n) pins, as illustrated in figure 3.9 b).

3.3.2.1 Operation Mode

At the beginning of each transition the master will select the slave using the SS line (the active SS line will move to the logical level 0). It will then generate the clock signal at a frequency less than or equal to the maximum frequency supported by the slave (usually in the order of MHz). In each clock cycle, the master sends 1 bit to the slave, checking the same in reverse. The transfers occur grouped in 8, 16 or 32 bits, depending on the slave [Lynch et al., 2016b].

There is no defined set of frequencies standard for the SPI protocol. However, frequencies are typically around 50MHz [Mishra et al., 2015]. For this speed the transfer rate will be 50Mbps. Since it is a full duplex communication, the effective transfer rate can reach 100 Mbps, if both master and slave are able to send meaningful information to one another [Mishra et al., 2015].

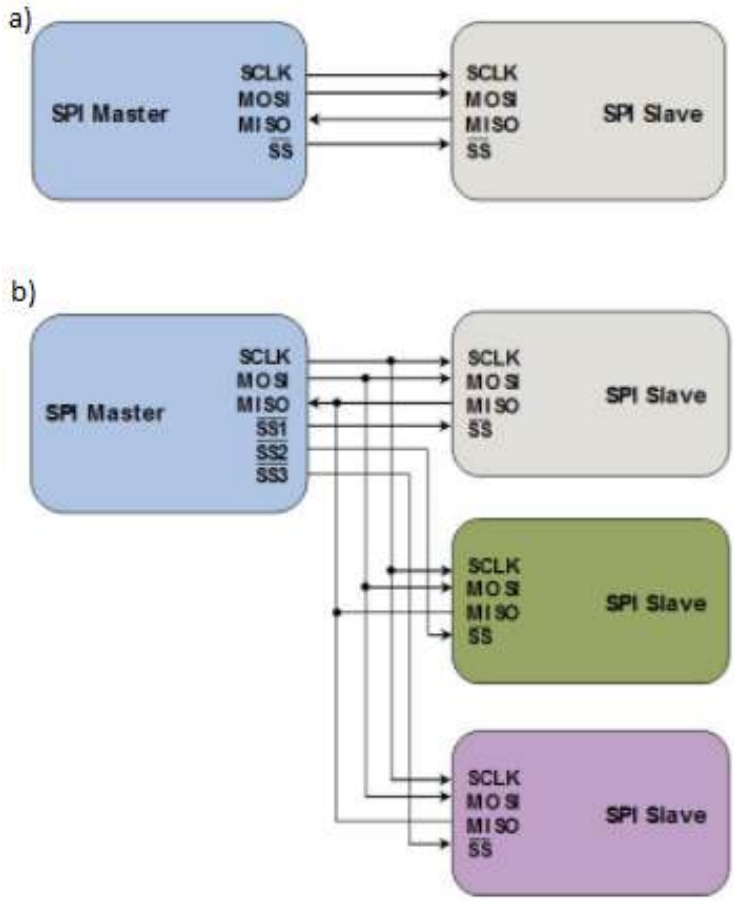

Figure 3.9: Example of two I2C bus configurations: a) shows a SPI master connected to a single slave; b) shows a SPI master connectedto multiple slaves [Leens, 2009].

3.3.2.2 Advantages and Disadvantages

The main advantage of the SPI protocol is that it supports higher frequencies compared to I2C, and therefore a higher data transfer rate. Since this protocol does not have a maximum limit for this parameter, as the case for I2C communication, this protocol is often used in sensors that present a greater flow of data, such as fingerprint sensors [Lynch et al., 2016b].

In the SPI protocol the full duplex communication is active by default, so if a situation occurs where both the master and the slave need to transmit information between them, this feature can be very useful.

In terms of complexity, the SPI and I2C protocol are both fairly simple. Unlike the I2C protocol, the SPI will not need pull-up resistors, so it will have a lower power consumption.

In SPI there is no limit on the address of slaves, as in I2C. Each SPI slave that is connected to the master will require the corresponding SS pin. This means that the number of pins required on the master device will increase depending on the number of connected slaves, as previously mentioned.

The main disadvantages of this protocol is that it does not have an acknowledgement mechanism to confirm receipt of data and does not present any flow control mechanism [Leens, 2009].

According to Mishra et al. [2015] there is no formal pattern in the SPI protocol, so there is no way to validate the protocol for a given product.

3.3.3 Overall considerations

Systems based on SoC (System on Chip) circuits, where a low number of pins is desirable for a greater simplicity of the integrated circuits, the I2C and SPI protocols are the most suitable since they allow the connection between several slave devices in a single controller. In terms of energy consumption SPI has an energy consumption lower than I2C, but compared to other protocols both are relatively small. Thus, it is not surprising that these two communications protocols are the most used in embedded systems.

Chapter 4

Implementation of the Measurement System

This chapter presents a proposal of a monitoring system for cycling. First is made a general description of the measurement system, where all its components are described, as well as is presented a description of all the hardware and software used in its implementation. Next are referred all the procedures that were required for the development of the system, from the detailed description of the firmware behaviour to the data migration to the Android platform.

4.1 System overview

The measurement system for evaluation of cycling performance developed in this dissertation consists of two main components: a smartphone (acts as central station) and two sensory nodes, physical devices, scattered in the body of the athlete. For the communication between the two entities involved in the system is used the BLE technology. Figure 4.1 illustrates the architecture of the monitoring system.

Figure 4.1: Architecture of the measurement system for cycling.

In our system the measurement and monitoring of the knee angle is the main focus, due to the extreme importance of this variable for the athlete. For this measurement, are used two devices with IMUs positioned on the athlete's thigh and shank, as can be seen in the figure above.

These devices have the function of collecting the movement data of the body segment in which it are placed, transmitting in real time to the smartphone and storing it in a memory card embedded in the device. Since it is active and outdoor monitoring there is some probability of BLE communication failures, however the data will be stored simultaneously, which allows a more detailed analysis by the coach/athlete at the end of each training session.

The sensory modules of the physical devices are composed by a set of three sensors, accelerometer, magnetometer and gyroscope, which will be described below. The IMU used presents a sensor fusion algorithm which allow to obtain data about its orientation, such as Euler angles. These describe the orientation of a rigid body in three-dimensional space. The three angles that describe the orientation of the device are Pitch, Roll and Yaw.

4.2 Description of the physical device

One of the main concerns when developing a device should be its size. This should be as small as possible to do not interfere with the natural movement of the athlete or to cause discomfort in the athlete. The dimensions of the developed devices are 82mm x 40mm x 22mm.

These devices can be divided into four different modules according to the functions they perform. A representation of its main components is shown in figure 4.2.

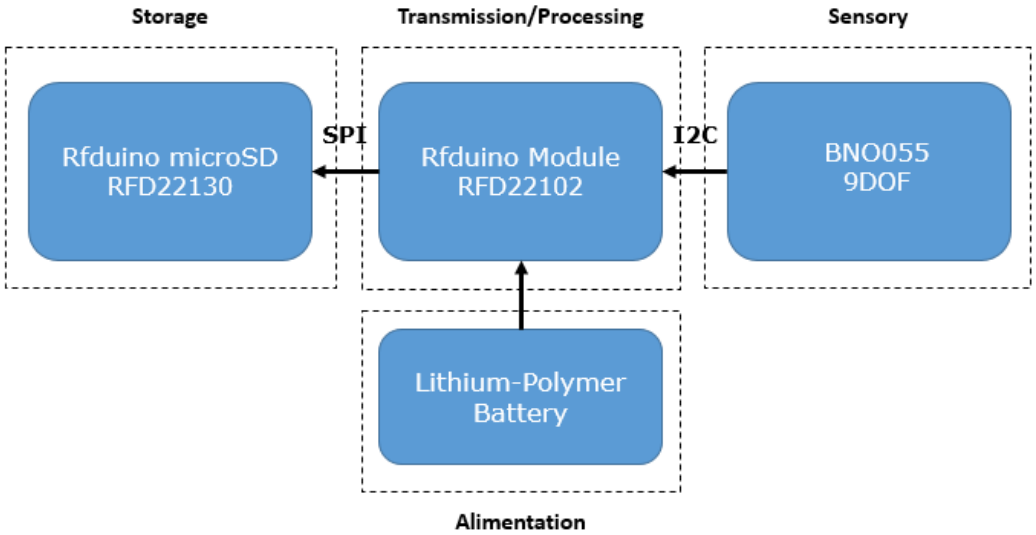

Figure 4.2: Schematic of the device main components.

1. **Transmission/Processing module**

This is the main module of the device, because it is here that all the code necessary for the overall operation of the system is implemented. The component that corresponds to this transmission module is Rfduino RFD22102.

Figure 4.3: Rfduino module.

RFduino is a Bluetooth 4.0 low power (BLE) module with built-in ARM Cortex M0 microprocessor that can be used in the development of several projects in a relatively fast and simple way. It is compatible with Arduino, which allows programming in Arduino Integrated Development Environment (IDE) software. The RFduino module require a USB-Shield, RFD22121, for its programming. Through Bluetooth communication with smartphones and tablets which have Bluetooth 4.0 version is possible to run a wide range of applications [RF Digital Corp, 2013].

This module has a 3.3V voltage regulator that allows not only powering itself, but also all other components in the circuit. The microcontroller presents ADC, SPI, I2C, UART communication interfaces and seven data input and output ports (GPIOs) [RF Digital Corp, 2013]. In table 4.1 are presented the main specifications of the Rfduino module.

RFduino Specifications	
CPU	16MHz ARM Cortex-M0
Flash memory	128kb
RAM	8kb
Supply Voltage	2.1V - 3.6V
Transmit Current	12mA
Receive Current	12mA
ULP Current	4μA
GPIO	7

Table 4.1: Main Specifications of RFduino

2. **Sensory module**

This module is composed of Adafruit's BNO055 system (figure 4.4). It consists of a tri-axial accelerometer, a tri-axial gyroscope, a tri-axial magnetometer and a high speed ARM Cortex-M0 based microprocessor to digest all the sensor data, in which is implemented a sensor fusion algorithm developed by Bosch Sensortec.

Figure 4.4: BNO055 inertial measurement unit.

The 3D accelerometer has a resolution of 14 bits, and the accelerometer scale range can be ± 2g, ± 4g, ± 8g or ± 16g, being defined when programming it. The data output rate can range from 8Hz to 1KHZ. The 3D gyroscope presents a resolution of 16 bits, the sensor scale range lies between 125 °/s to 2000 °/s and the data output rate can range from 12 Hz to 523 Hz. The magnetometer presents a range of ± 1300 μT (axes x, y) and ± 2500 μT (z axis) and a resolution of ≈ 0.3 μT [Sensortec, 2014].

This 9DOF IMU presents a 100Hz maximum sampling frequency, allowing acquire up to 100 samples per second. The BNO055 architecture is illustrated in figure 4.5.

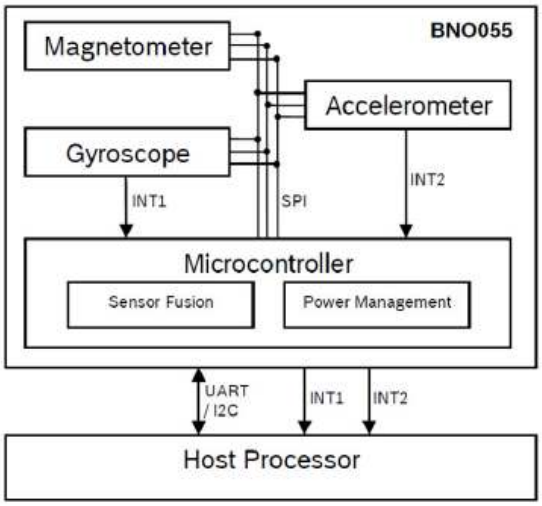

Figure 4.5: BNO055 architecture [Sensortec, 2014].

One of the main difficulties, when using inertial measurement units in which the data of the accelerometers, gyroscopes and magnetometers are obtained separately, is the obtaining of 3D space orientation. The BNO055 with integration of the sensor fusion algorithm allows to merge the data of the three sensors and thus to obtain instantaneously absolute orientation values like the Euler angles or the quaternions.

The BNO055 can have different outputs, according to what the user intends for a given project. In this specific case the output will be the absolute orientation of each device, through the Euler angles in degrees. As interfaces for digital bidirectional transmission the BNO055 presents the

I2C and UART protocols. This module will communicate with the processing module, Rfduino, through the I2C protocol, as illustrated in figure 4.2.

3. **Storage module**

This module will serve to store all the data sent by the sensory module to the processing module. For this purpose is used the RFD22130 MicroSD Shield, with a 8GB microSD memory card. Communication with the RFduino is performed via the SPI protocol.

4. **Alimentation module**

The entire circuit is powered by a 3.7V and 400mAh lithium-polymer rechargeable battery. At this stage the battery used has a duration of about 4 hours, which allows continuous monitoring throughout the training session.

4.3 Firmware Development

The development environment used was the Arduino IDE. This is an open-source software that allows the creation of various programs in a simple way. Programming in Arduino software is based on C/C++ programming languages. It is compatible with Windows, Mac OS X and Linux operating systems and can be used with any Arduino board, including Rfduino.

In a first phase was developed a program that was implemented in the microprocessor, Rfduino, whose function is to receive the data collected by the inertial unit, and then send them in both directions, via BLE to a smartphone and to the microSD card using SPI protocol.

4.3.1 Firmware Operation

The program starts with initialization of the variables and libraries used in code development. The first function to call is void setup (), being executed only once. It is at this stage that the program checks if the IMU is operational, checking if the I2C connections are correct. If so, the program will check if the SD card is inserted and working correctly. If this condition is verified a .csv file will be created to store the data coming from the IMU. If the SD card is not detected, the program continues its operation, however the data is not stored. If the BNO055 is not operational, the program cannot advance, leading to the closure of the program.

Next the program will advance to the void loop () function. At this stage, the RFduino will be continuously receiving the values of the Euler angles collected by the IMU, with a delay between sensor readings of 20 ms. Then the program will check if the condition that led to the creation of a csv file is verified.

Since RFduino has the capacity to send 20-byte packets, it was decided to define the Euler angles values as float data (4 bytes), which allows to send all the data in a single packet. After placing the collected data into packets, they will be sent by BLE technology to the smartphone, through the *RFduinoBLE.send()* function, and to the SD card by SPI protocol.

If interruptions occur in BLE communication for some reason, the program will continue to send data but only to the memory card, leading to loss of data in real time. As soon as the BLE communication becomes available again, the transmission to the smartphone is re-enabled.

At any time, the user can send the STOP command in order to finish the data reception. The flowchart representing the developed program is illustrated in Figure 4.6.

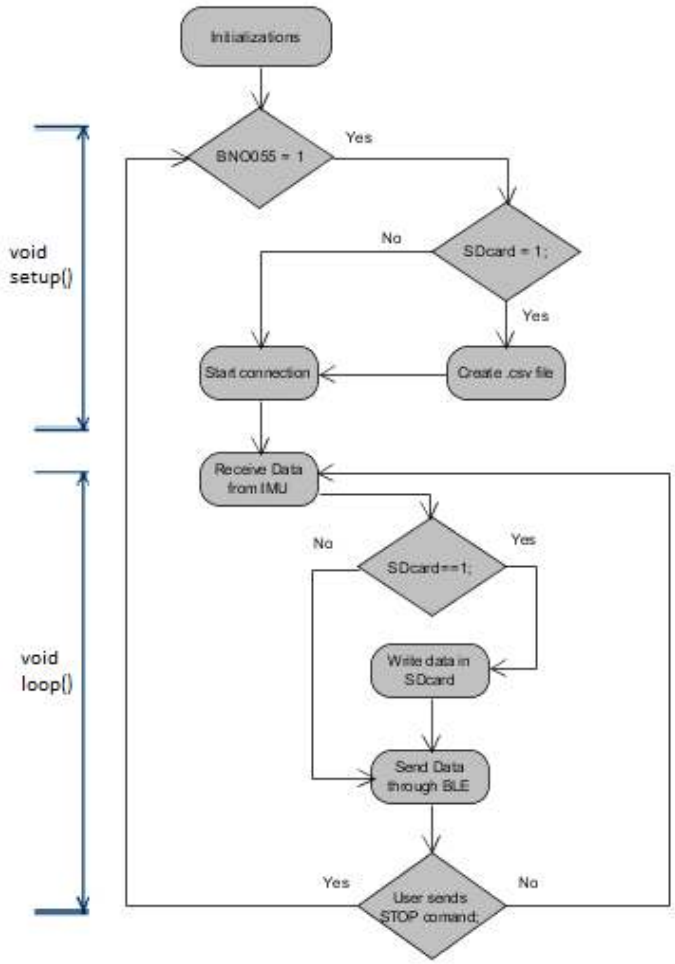

Figure 4.6: Fluxogram of the program developed in Arduino.

4.4 Android Application

After the design of the physical device, it was necessary to develop an interface that would allow a simple and practical visualization to the user. For this purpose an Android application was developed, called "CyclingTracker". This app will periodically receive information from the sensory nodes, allowing the athlete to have real-time visual feedback regarding the knee flexion angle along the course.

For the implementation of CyclingTracker the development software used was Android Studio. This is based on JetBrains IntelliJ IDEA Software and was made specifically for the creation of

Android applications. The programming language is Java and is compatible with the Windows operating systems, Mac OS X and Linux and has replaced the Eclipse Android Development Tools (ADT) as Google's primary IDE of native development for Android.

Android is a mobile operating system based on Linux and developed by Google that appeared in the year 2007. Since its emergence, has captured the interest of several companies, app developers and users in general. It is currently the most widely used operating system worldwide and its constant upgrades allow not only the enhancement of various features but the increase of supported hardware. Its main advantage is to be an open-source platform and to be increasingly available for a wide range of devices. Currently Android OS is in version 8.0 Oreo. Support for Bluetooth Smart Ready devices was possible from Jelly Bean version 4.3, allowing the implementation of BLE communication between multiple devices.

The developed application called "Cycling Tracker", aims to monitor the athlete's posture during a training or competition event. The application is executed on the smartphone, which assumes the role of central station and serves as interface with the user, in this case, the athlete. The app periodically receives the information collected by the sensory nodes, placed on the athlete's thigh and shank, and with these data, after appropriate treatment, calculates the knee flexion angle of the athlete. At this stage of development, the application is not intended to indicate whether the athlete at any given time has the correct posture or not, but has the ability to indicate in real time the athlete's knee flexion angle along the route.

The application, being designed to run at the central station, must meet certain typical requirements of a WSN and, of course, requirements at the level of the posture monitoring system in question. With respect to the functional aspects desired for a WSN, the application should be: scalable, allowing support for several sensory nodes; bear a debit required for delivery of the data generated by the application; ensure reliable data transmission in a real-time context; secure a low power consumption, which will depend on the amount of data sent, the frequency at which they are sent and the number of nodes connected to the central station.

With regard to the main requirements of the developed application, it must be able to connect to the two sensory nodes via BLE and periodically receive their information. For the correct functioning and accuracy of the values measured by the sensors of each module, a previous calibration of them is necessary. With the two devices belonging to the system connected and their sensors properly calibrated, the application must be capable of calculating the orientation of the monitored body segments and presenting in real time the variations on the knee flexion angle to the athlete. The calculation of this angle starts when the athlete begins his training session, allowing a visual feedback on his cycling performance along the course.

4.4.1 BLE API for Android

As previously mentioned, the communication technology used in the sensor network of the measurement system is BLE. This technology has the advantage of being compatible with the hardware and software of most of the latest smartphones, allowing an increase of applications in wearable monitoring systems.

In addition to the emergence of BLE, Google has made available an API for Android, in order to implement the methods and features of device discovery, connection establishment and activation of notifications to receive the data.

In the developed system the central station, which executes the application, has the role of master and the sensory nodes play the role of slaves. For the roles defined by the GATT layer, the sensory nodes play the role of GATT Server, since they contain the service implementation and all data to be sent to the central station, while the smartphone (central station) plays the role of GATT Client, because it periodically receives the data collected by the sensory nodes, that is, it benefits from the service implemented in the GATT Server. Figure 4.7 shows the distinction between the roles played by both intervening entities of the system.

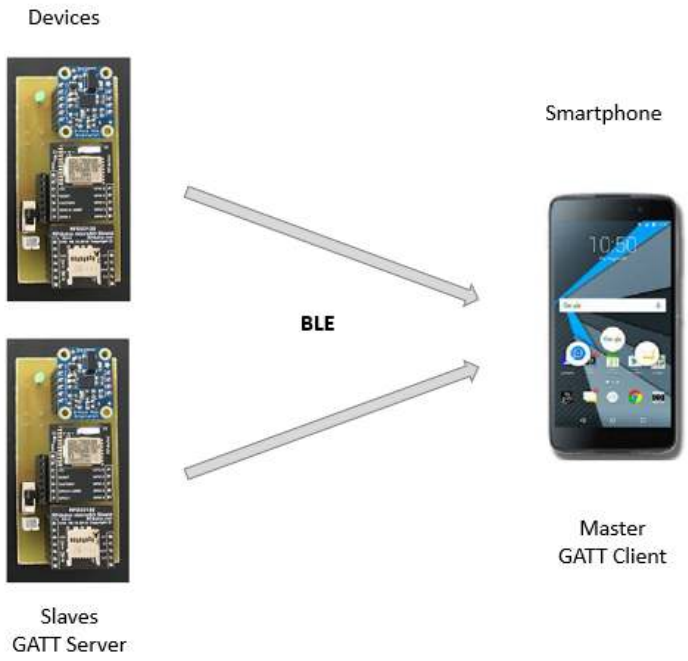

Figure 4.7: Roles of the entities involved in the system.

For the implementation of BLE technology in the application (GATT Client) was used a set of methods available in a standard application, provided by Google in the Android Developers portal. This function had as basic functions, the establishment of the connection to a GATT Server and reception of data. The methods associated with these tasks are included in a service called BluetoothLeService.

In order to take advantage of Bluetooth capabilities in the application, it was necessary to declare the respective permissions in the application manifest. Without these permissions, the app would not be able to make any Bluetooth communication, such as requesting a connection, accepting a connection, and transferring data. Was declared a specific permission to allow only BLE-compatible devices to be found. Figure 4.8 represents the permissions implemented in the manifest.

```
<uses-permission android:name="android.permission.BLUETOOTH" />
<uses-permission android:name="android.permission.BLUETOOTH_ADMIN" />
<uses-feature android:name="android.hardware.bluetooth_le" android:required="true" />
```

Figure 4.8: Bluetooth permissions.

For BLE communication to be possible, the user must first activate the Bluetooth of the smartphone. If this condition is not ensured the application will not move forward. The BluetoothAdapter object is required in all activities that benefit from the Bluetooth service. Represents the Bluetooth adapter (radio interface) of the device itself, and through it the application can interact with Bluetooth. After this, the StartLeScan() method is used in order to begin the discovery of the devices. This is an exhaustive process for the battery, and therefore, it is automatically suspended after 10 seconds, long enough to find the sensory nodes of the system. Using the getName() and the getAddress() methods, the program will get the name and the address of the existing devices, and if it matches to the previously defined the connection is immediately established through the connectGatt() method.

4.4.2 Design and Architecture

One of the main concerns when developing the android application was to develop a user-friendly app and that it be able to present the desired results in real time. Thus, the application has only three interfaces, in which the first one is simply a welcome presentation. The second interface is relative to scan for devices and connection establishment operations. These two interfaces are shown in figure 4.9.

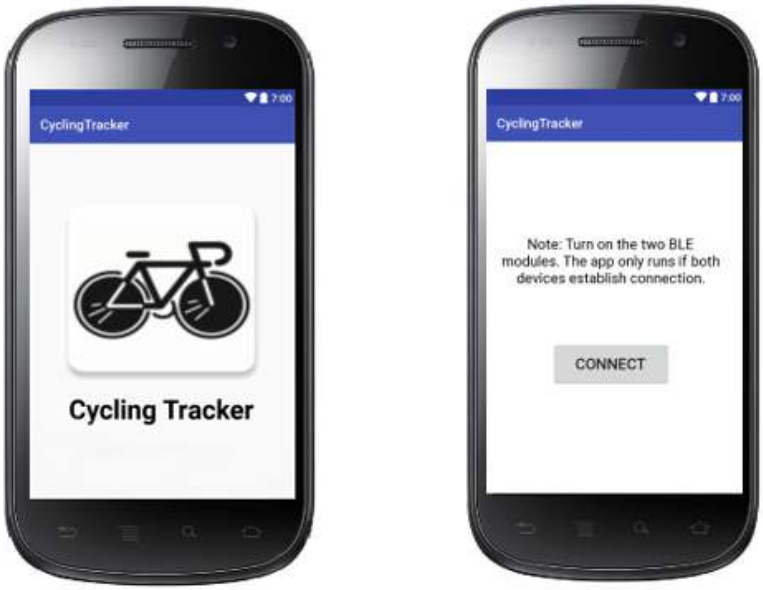

Figure 4.9: a) Welcome interface; b) Connection interface.

The third and main interface of this application is illustrated in figure 4.10, and was conceived with the aim of providing to the user the results of his knee flexion angle along the path.

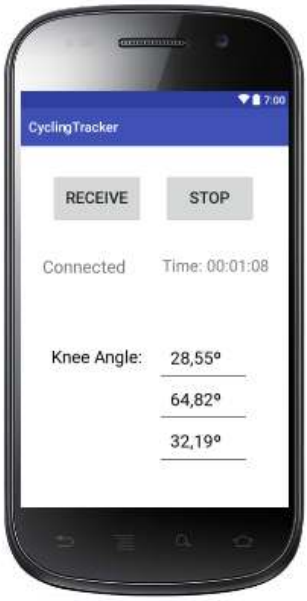

Figure 4.10: CyclingTracker main interface.

In order to describe the main functionalities of our application and its interaction with the users we created the use-case diagram represented in figure 4.11.

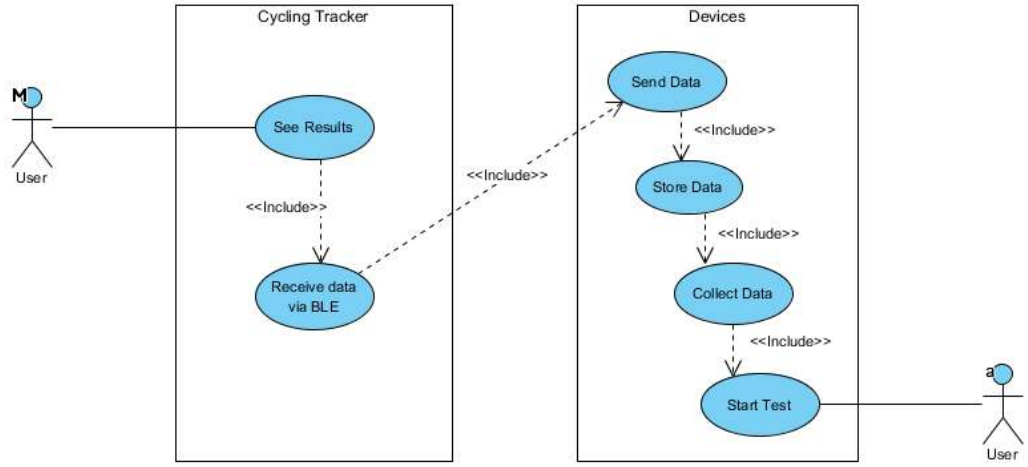

Figure 4.11: Use Cases Diagram.

The application in a general way will allow the user to visualize the results obtained with the continuous monitoring of the knee joint during cycling. The devices in addition to sending the

data via BLE to the application will also store the collected data into an internal memory, allowing a deeper analysis in the future.

For a better understanding of the application architecture, was also developed an activity diagram, shown in figure 4.12.

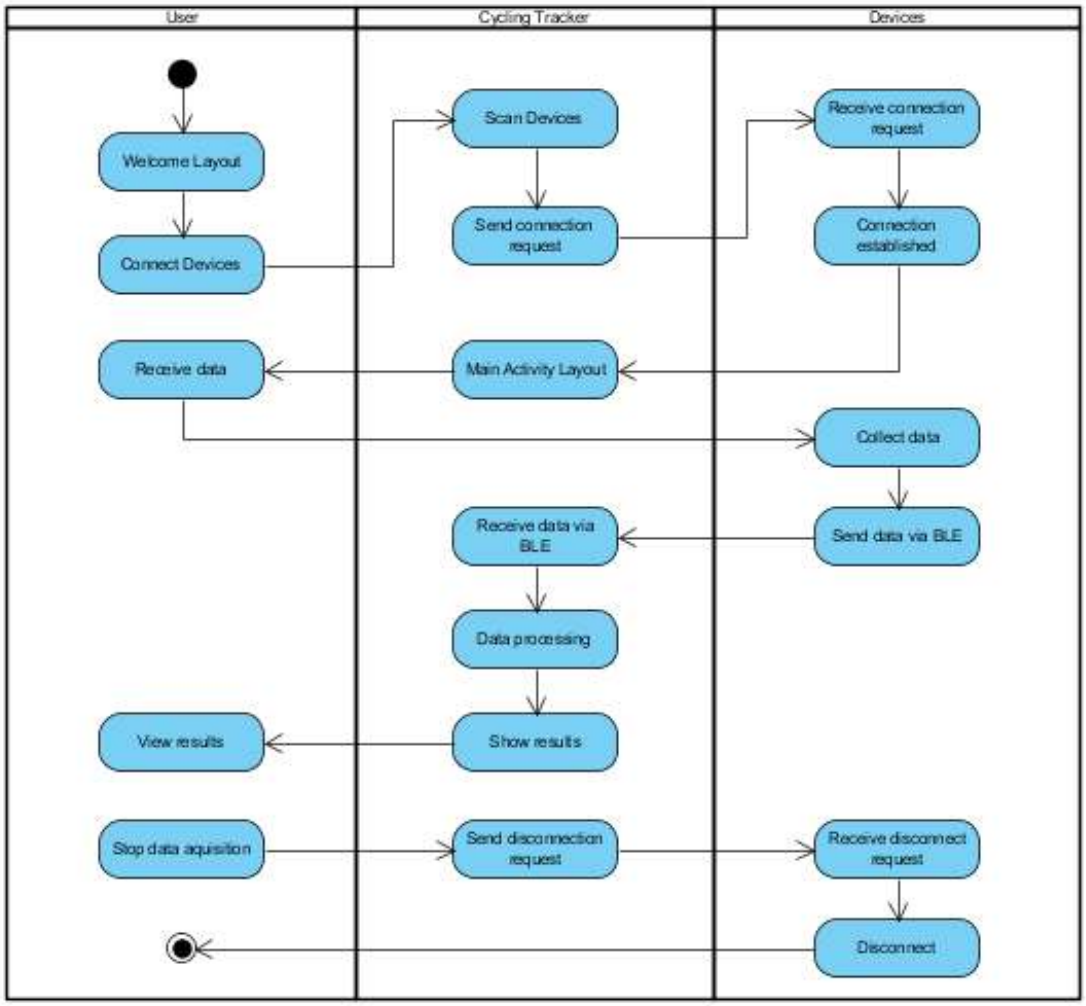

Figure 4.12: Workflow Diagram.

The application starts by presenting to the user its welcome interface. Then is presented the second interface, where the discovery process of BLE devices is started. In this interface is shown to the user a note to turn on the physical devices. After that the user must then press the "Connect" button to establish connection between the app and the sensory nodes. All processes until the connection establishment are described in the previous section.

After establishing the BLE connection with the two devices the user will enter in the main interface of the app, which corresponds to figure 4.10. At the moment of initiation of the training or test session the athlete must press the “Receive” button in order to start the data transmission between the sensory nodes and the application. The app will then combine the collected data and with due processing calculate the knee flexion angle of the athlete along the course. In order to

provide a simple visualization of this parameter to the user the results are displayed numerically in a ListView. At the end of the training session the athlete must press the "Stop" button in order to end the data transmission.

4.5 Knee Angle Estimation

In geometry, the orientation, also called attitude, of an object, is part of the description of how this object is placed in space [Diebel, 2006]. Through the combination of the information provided by the IMU, using sensor fusion algorithms, one is able to calculate and estimate the orientation of an object.

Sensor fusion methods combine sensory data in a way that should ideally give better performance than that achieved when each source of information is used alone [Oliveira, 2017]. The design of systems based on sensor fusion methods requires the availability of complementary sensors in order that the disadvantages of each sensor are overcome by the advantages of the others [Ligorio and Sabatini, 2013].

If the gyroscopes provide perfect measurements of the IMUs turn motions, then with simple integration of these signals would be possible to estimate the attitude [Oliveira, 2017]. However, IMUs gyroscopes suffer substantially from noise and drift, and for that reason, other sensors like accelerometers and magnetometers are needed to correct this imperfectness. Thus, to get the best estimate of the IMU attitude, is needed a sensor fusion algorithm that combines the measurements from the different sensors, providing a more useful result witch combined the strengths of each sensor [Fux et al., 2008].

3D joint angular kinematics requires the estimate of the 3D sensor's orientation in space. Therefore, these solutions are based on sensor fusion algorithms of IMU signals and most of them feature the use of a magnetometer [Picerno, 2017]. In some cases the sensor orientation is readily furnished by proprietary "blackboxed" sensor fusion algorithms provided by the manufacturer of the sensor [Picerno et al., 2008] [Cutti et al., 2010], while, in other cases, the sensor orientation algorithm was proposed by the researchers and explained in the papers [Favre et al., 2009] [O'Donovan et al., 2007].

Over the years many algorithms and techniques have been suggested for IMU-based knee angle estimation. Despite the variety of approaches, the vast majority of authors defines the flexion/extension angle of the knee joint as the angle between the upper and lower leg along the main axis of relative motion, this is, the knee joint axis [Liu et al., 2009] [Takeda et al., 2009] [Favre et al., 2008] [Cooper et al., 2009]. In other words, the projections of the upper and lower leg into the joint plane, to which the joint axis is normal, confine this angle [Seel et al., 2014].

According to Seel et al. [2014] the simplest approaches in the literature assume that the IMUs are attached such that one of the local coordinate axes is aligned with the joint axis. Integrating the difference of the upper and lower sensors will yield a drifting flexion/extension angle.

As mentioned previously, some inertial sensors include on-board orientation estimation, which is usually based on a sensor fusion of the acceleration, angular rate and magnetic field vector

measurements. These estimates describe the orientation of the sensors with respect to a fixed reference coordinate system, either in quaternions, rotation matrices or Euler angles [Seel et al., 2014].

Our system is equipped with sensors that presents a sensor fusion algorithm which allow us to obtain orientation estimation values directly, as the Euler angles. The coordinate system used to calculate the orientation of the angles is shown in Figure 4.13. Pitch defines the rotation on the x-axis, Roll the rotation on the y-axis and Yaw the rotation on the z-axis.

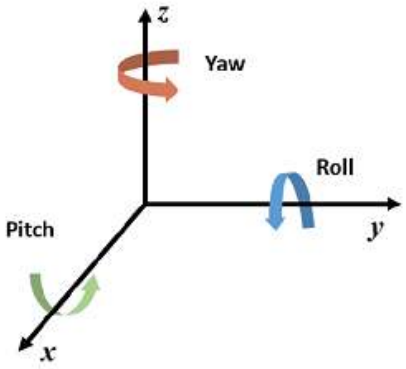

Figure 4.13: Euler angles representation in a coordinate system.

The two sensory nodes constituent of the measurement system are placed to measure the athlete's knee angle. For this measurement, one device is placed on the upper leg (thigh) while the other is placed on the lower leg (shank), thus simulating the effect of a goniometer. According to Maio [2014] the angle between the two referred body segments is given by equation 4.1.

$$A_{knee} = \cos^{-1} \frac{\vec{V}_{\text{upperleg}} \circ \vec{V}_{\text{lowerleg}}}{||V_{upperleg}||||V_{lowerleg}||} \tag{4.1}$$

For the calculation of the VupperLeg and VlowerLeg vectors, the Pitch, Roll, Yaw values of each sensory node are removed at each moment and multiplied by the rotation matrix, to obtain the orientation of each sensory node. The knee joint motion is determined by the orientation of each segment and is described in the XYZ-Euler angle representation. The rotation matrix that transforms the sensor frame at any time step into the initial sensor frame is defined by the multiplication of the single rotation matrices around each axis and is determined by:

$$R_i = \begin{pmatrix} c\theta c\psi & -c\theta s\psi & s\theta \\ c\phi s\psi + s\phi s\theta c\psi & c\phi c\psi - s\phi s\theta s\psi & -s\phi c\theta \\ s\phi s\psi - c\phi s\theta c\psi & s\phi c\psi + c\phi s\theta s\psi & c\phi c\theta \end{pmatrix} \tag{4.2}$$

where c and s represents the cos and sin functions and ϕ, θ and ψ are the rotation angles around the x, y and z axes respectively [Jakob et al., 2013].

The knee angle obtained by the equation 4.1 presents as maximum value 180 degrees when the flexion of the leg is nil, that is, fully stretched, and as the athlete loads the leg, the value of this angle decreases [Maio, 2014]. This means that the result obtained by this method is related to the extension angle and not to the flexion angle. In our system it is considered that when the athlete presents the leg fully stretched, the resulting knee flexion angle is equal to 0 degrees. Thus to estimate the athlete's knee flexion angle as intended, the value obtained through the equation 4.1 is subtracted to 180 degrees, since the flexion/extension angles are complementary to each other.

Chapter 5

Results and Discussion

In this chapter the experimental tests carried out and the results obtained through them are presented and discussed. The tests were performed by an athlete in a natural training environment, outdoor conditions. Two different configurations were tested on the placement of the devices in the lower limb of the athlete, allowing a comparison. All the graphics obtained with both tests are presented below.

5.1 Experimental Tests

The experimental tests were performed by a recreational athlete in outdoor conditions in order to allow a monitoring in a real training or competition environment. The trials were conducted to proof of concept of the developed measurement system for cycling evaluation. The athlete performed a series of different tests with the measurement system mounted on his right leg, from static measurements to real cycling activity measurement trials.

During data collection throughout the experimental tests conducted, the smartphone, which functions as the central station of the system, was positioned on the bicycle in order to provide the athlete with visual feedback, as shown in figure 5.1.

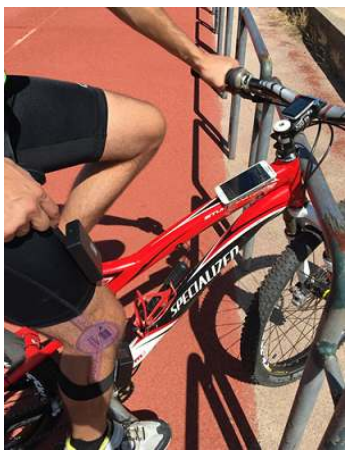

Figure 5.1: Smartphone position on the bycicle.

Recent studies have reach a consensus in recommending an optimum saddle height for trained and untrained cyclists of 25-35° knee angle at the lowest point of the pedaling cycle. With the knee flexion angle in the range mentioned the athlete will improve his performance and reduce the knee injury risk associated with the practice of this sport [Bini et al., 2011] [Peveler and Green, 2011] [Alencar and Matias, 2009]. For the correct positioning of the cyclist on the bicycle during the experimental tests and data collection with the developed system, a goniometer was used to ensure that the saddle height of the bicycle was correctly adjusted to the athlete.

A goniometer is an instrument used in medicine and in rehabilitative programs, like physical therapy or athletic training, which measures range of motion joint angles of the body. This instrument represents a clinical tool that allows objective measurements in order to track progress in rehabilitation programs. The goniometer, see figure 5.2, is one of the most widely used evaluation procedures for joint angle measurements and can be considered a fundamental part of physical therapy.

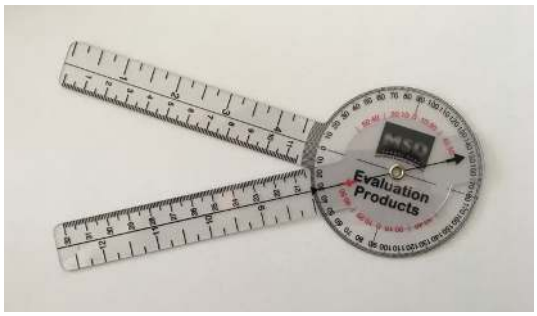

Figure 5.2: Goniometer.

The main advantages of this method include the low cost of the instrument and the fact that it is easy to use for measurement of knee joint angle. Unlike camera motion tracking systems, the used manual goniometer does not allow a continuous measurement, so it was used for static measurements in order to validate the measurements obtained by the developed system.

In the literature, both configurations of the sensory nodes, frontal and lateral, were tested by several researchers in their investigations for estimating the knee angle [Tannous et al., 2016] [Tognetti et al., 2015] [Jakob et al., 2013] [Marin-Perianu et al., 2013] [Maio, 2014]. Thus, it was tested both dispositions, for comparative purposes in order to analyze which configuration presents better results for the variation of the knee flexion angle of the athlete during cycling.

The data recorded during the experimental tests were then transferred to the computer at the end of the collection, for a more detailed analysis. Matlab software was used in order to import and process the data obtained through the collection performed by the two physical devices, in order to represent graphically the tracking of the athlete's knee angle along the course.

5.1.1 Test A

In this first trial, was tested the lateral configuration of the physical devices, data were collected with the devices placed on the lateral side of the athlete's thigh and shank (see figure 5.3). This

test has as main objective the study of the knee flexion angle range of the athlete during cycling. Inertial data were extracted from the sensory nodes in order to be able to measure this parameter, and to give feedback to the user.

Figure 5.3: Anatomical placement of the devices, lateral configuration.

Figure 5.4 illustrates the physical device's coordinate system as well the euler angles representation. The front of the orientation of the module is on the z-axis, where Pitch defines the rotation on the x-axis, the Roll on the y-axis and the Yaw on the z-axis.

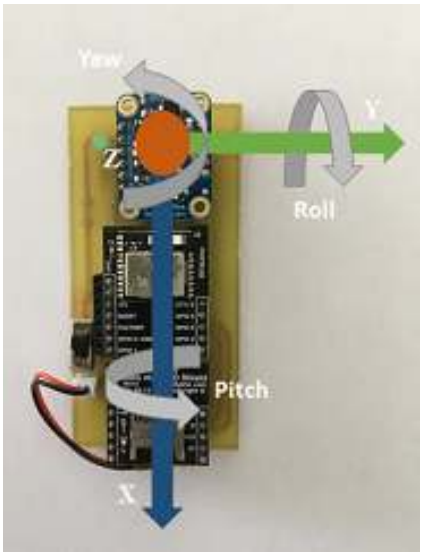

Figure 5.4: Physical device's coordinate system.

Next, the various graphics obtained through the inertial data collected and stored on the memory card will be displayed. As previously mentioned the Matlab software was used for the data

treatment.

In figure 5.5 can be seen the graphics of the euler angles obtained by the two sensory nodes. The upper graphic is relative to the IMU placed on the thigh, and the lower graphic is relative to the IMU placed on the shank of the athlete.

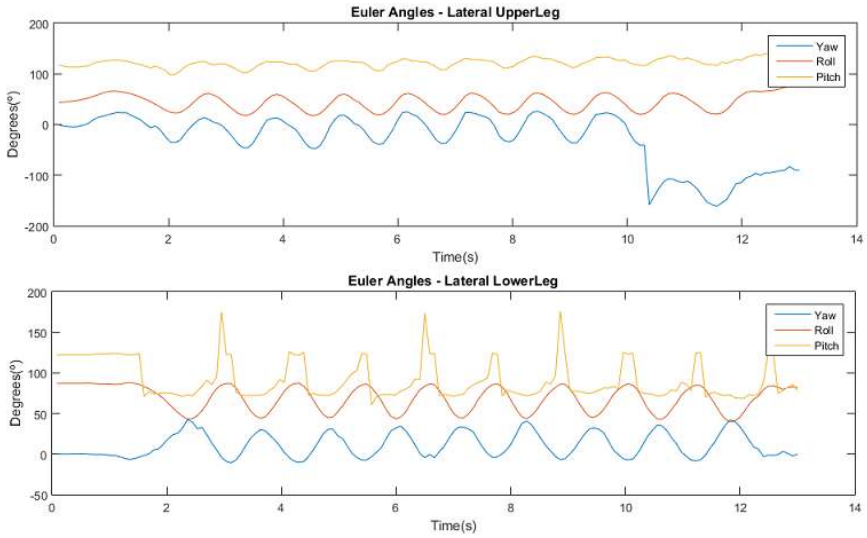

Figure 5.5: Graphics of the Euler angles during cycling.

As expected, through the visualization of the graphs obtained it is possible to observe that the sensor placed on the athlete's shank shows a greater rotation about their axes, especially in the pitch angle, compared to the sensor placed in the thigh.

Through observation of the variations presented by the euler angles during cycling, it is easily observable repetitive patterns of movement (see figure 5.5), which represents the athlete's pedaling cycle along the course.

Figure 5.6 shows the graph corresponding to the knee angle flexion interval of the athlete during cycling practice, estimated with the lateral configuration, and obtained through the combination of the inertial data collected by the two IMUs.

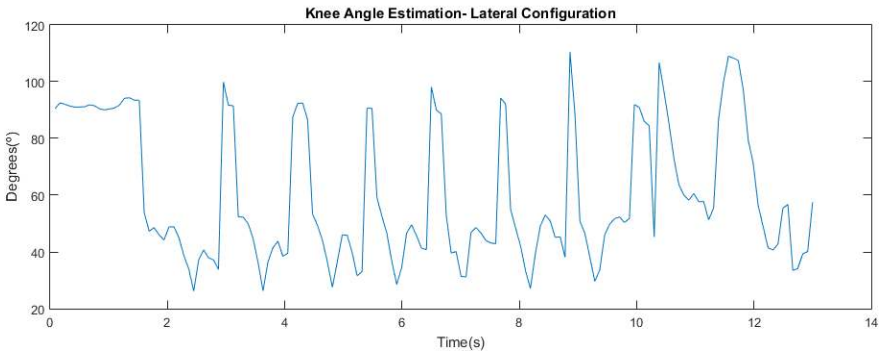

Figure 5.6: Knee Angle Estimation with lateral configuration.

The goniometer were used to quantify the baseline limitations of knee angle motion during cycling activity, and with this measurements was possible to report that the flexion range of the knee angle varies between 25 to 120 degrees with the pedaling movement.

With the observation of the graph relative to the variation of the knee flexion angle during cycling, figure 5.6, it is possible to verify that the athlete's knee angle presents a behavior close to the expected, through the goniometric measurements previously performed.

5.1.2 Test B

In this second trial, was tested the frontal configuration of the physical devices, data were collected with the devices placed on the athlete's thigh and shank frontally (see figure 5.7). This test has as main objective the study of the knee flexion angle interval of the athlete during cycling. Inertial data were extracted from the sensory nodes in order to be able to measure this parameter.

Figure 5.7: Anatomical placement of the devices, frontal configuration.

As previously mentioned was used Matlab software for data treatment, allowing a more detailed analysis of athlete's behaviour during cycling. For this purpose, the inertial data stored on the memory card of both physical devices was used.

Figure 5.8 shows the graphics of the euler angles obtained by the two sensory nodes. The upper graphic is relative to the IMU placed on the thigh, and the lower graphic is relative to the IMU placed on the shank of the athlete.

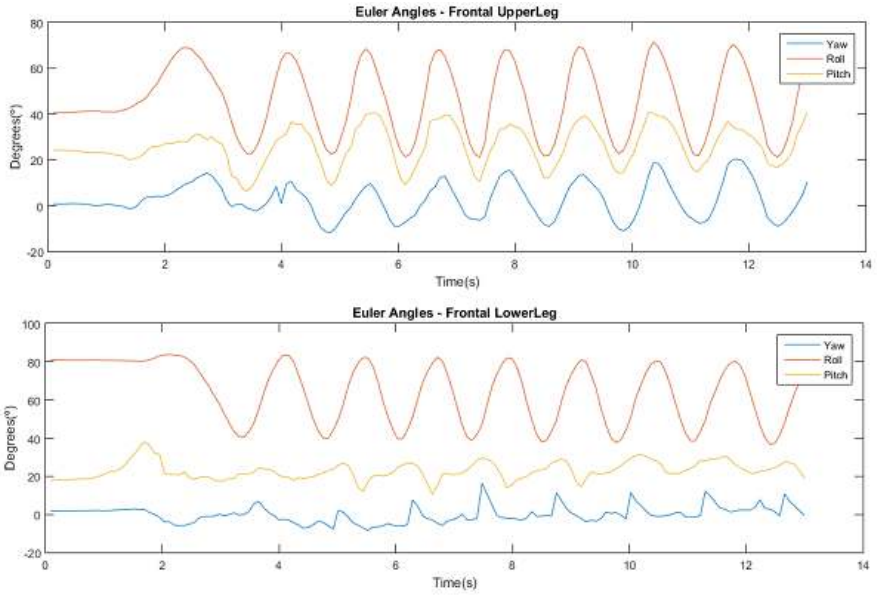

Figure 5.8: Graphics of the euler angles collected with frontal configuration during cycling.

Through the visualization of the graphs illustrated in figure 5.8, it is possible to observe that the sensor placed on the athlete's shank shows a greater rotation about their axes, especially in the pitch angle, compared to the sensor placed on the thigh. Rotation around the y and z axis, roll and yaw, behaves similarly between the two devices placed on the athlete's leg.

Regarding the behavior of the euler angles obtained during this test, illustrated in the graphs of figure 5.8, repetitive patterns of movements alluding to the pedaling cycle are not so easily observed compared to the graphs of the euler angles obtained in test A.

In figure 5.9 can be seen the graph corresponding to the variation of athlete's knee flexion angle during cycling practice, estimated with the frontal configuration, and obtained through combination of the inertial data collected by the two IMUs.

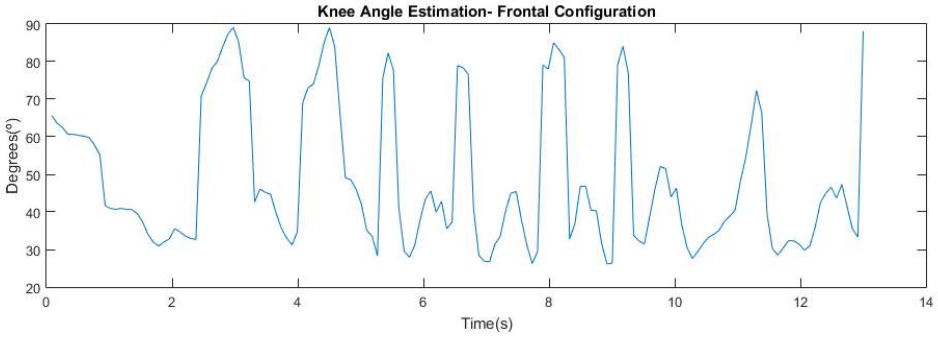

Figure 5.9: Knee Angle Estimation with frontal configuration.

The results obtained with this test demonstrate a great variability on the athlete's knee flexion angle during the cycling practice. As can be seen in Figure 5.9, the frontal disposition of the

devices in the athlete's leg led to less satisfactory results in the variation interval of the knee flexion angle during cycling than those produced with lateral configuration, performed in test A.

Through this more detailed analysis implemented on this chapter, and with the observation of the obtained graphics resulting from the experimental tests, is possible to verify that several relevant parameters for the athlete's performance can be analyzed: the tracking of his knee joint angle behavior during the trial, the assessment of his pedaling movement and technique and obtain information regarding to his body positioning on the bicycle.

If the variation of the knee flexion angle is between 25 and 35 degrees at the lowest point of the pedaling cycle, then the athlete is correctly positioned on the bicycle and the saddle height is well adapted to the athlete's body [Bini et al., 2011]. The verification of this factor, as can be observed in figure 5.6, will allow the athlete to improve his performance and reduce the injury risk.

Two configurations were tested in the disposition of the sensory nodes on the athlete, allowing a comparison between the measurements performed by both. Through the results obtained with these tests, it was possible to verify that the disposition of the physical devices in the lateral face of the athlete's right lower limb led to more satisfactory results on the calculation of the knee joint flexion angle during cycling than the results obtained with the frontal disposition.

The use of Euler angles for attitude estimation are popular because they are easy to use and provide a level of intuitive understanding, however they present some singularities. These singularities found in the Euler angles arises from the gimbal lock [Diebel, 2006]. This effect results from the indistinguishability of changes in the first and third Euler angles when the second Euler angle is at some critical value. These singularities can cause some errors in the results obtained on the knee angle calculation.

The method used in this investigation is not consensual, much due to the singularities and ambiguity that the Euler angles presents. According Diebel [2006] when is necessary to integrate incremental change in attitude over time Euler angles are less accurate than unit quaternions.

Chapter 6

Conclusions and Future Work

It is essential for any cyclist to optimize his pedaling movement in order to maximize the performance and minimize the risk of overuse injuries. Nowadays motion analysis systems had become an important tool for athletes, however, most of them are very expensive and only can be used on laboratory environments. Ambulatory motion analysis systems based on MEMS inertial units allow the continuous monitoring in real outdoor environments.

In cycling there are not many systems developed with this scope to evaluate and monitor the athlete's movement compared to other sports. There is a need in cycling for portable systems that can continuously monitor the kinematics of the cyclist, process the data collected and provide real-time feedback that can be used to improve the athlete's performance.

This dissertation aimed to contribute to the monitoring and rectification of the posture of cycling athletes, since their performance is strongly influenced by it, thus helping to increase control over their physical activity. For this purpose, sensors were scattered on the athlete's lower limb and the collected data combined for monitor the knee joint flexion angle in real time, using a measurement system for monitoring the posture, orientation and movement of the athlete based on sensory nodes.

With this study was developed a measurement system for cycling evaluation that allow to the user real-time feedback but also a more detailed analysis at the end of the training session. The measurement system offers an appealing solution to analyze the evolution of the lower limb kinematics over time. The system could be used to detect alterations of the athlete's pedaling technique, so that cyclists can adjust their pedaling movement for maintaining a high level of performance and limit the risk of overuse injuries during cycling.

The developed measurement system allow to athletes obtain a continuous monitoring of their body positioning on the bicycle, a continuous monitoring of their pedaling movement, orientation and technique, and a tracking of their knee flexion angle behavior during cycling. All these factors that our system can measure have direct influence on the cycling performance, so, the use of this measurement system by athletes can improve their training methodologies and consequently optimize their performance.

Initially was started the development of the physical devices, these are made up of three main

modules that enable the collection, storage and transmission of sensory data. Algorithms were implemented in these devices in order to perform the mentioned functions.

In order to provide the athlete with real-time feedback of his knee flexion angle during cycling and consequently his positioning in the bicycle, an Android application was developed that would be incorporated into a smartphone, which served as system's visual interface. The data transmission between the two entities of the system was implemented through BLE technology. Currently, this technology presents an exponential growth in monitoring systems in the sports area. In addition to the low power consumption, it has a topology that allows the incorporation of several types of sensors.

The experimental tests were performed by an athlete with the measurement system devices placed on his thigh and shank. In order to properly positioning the athlete on the bicycle, the saddle height was adjusted through the use of a goniometer. Two different dispositions of the sensory nodes, lateral and frontal, were tested in order to compare the measurements made between these two configurations. The lateral disposition of the physical devices presented better results relative to the knee joint angle behavior during cycling.

Although these devices, within the framework of this dissertation, are implemented on the practical case of cycling, they present characteristics that make it easily to be applied in another sport activity, whose study of motion captured by inertial units has some utility. The IMUs incorporated on the system has characteristics that allow it to obtain different outputs, from reading raw data of the sensors to estimating orientation values through the measurements of the three sensors, which can be used to measure other pertinent parameters on another sport context.

This dissertation consisted on the implementation and development of a prototype of a monitoring system for cycling. For athletes and coaches to obtain a deeper knowledge of all these parameters mentioned above, will allow to improve their training methodologies and contribute to the optimization of the athlete's cycling performance.

There are future improvements to be made to the system in order to improve and complement the work developed. The size of the physical devices can be further reduced, allowing a better adaptation to the body of the athlete and consequent reduction of the discomfort caused by them. The inclusion of more physical devices on the system is also another possible improvement, in order to allow an increase of the output parameters, since they could be placed in different body positions, allowing, for example, the calculation of the symmetry between the lower limbs behavior during cycling.

It would also be relevant to calculate other variables such as the instantaneous velocity or the pedaling cadence of the athlete during cycling, since these parameters are also important in the evaluation of the athlete's performance, and thus the development of algorithms capable of calculating these variables during cycling, which would complete the measurement system. Another factor to take into account as future work would be to implement a method to estimate the athlete's knee flexion angle based on quaternions values, due to the fact that these do not present the singularities of the Euler angles.

The Android application can also be improved, allowing the direct visualization of more parameters of interest and the incorporation of a database, in order to store several sessions of training per athlete, would also be an important complement in the improvement of the system.

Bibliography

Norhafizan Ahmad, Raja Ariffin, Raja Ghazilla, and Nazirah M Khairi. Reviews on Various Inertial Measurement Unit (IMU) Sensor Applications. 1(2):256–262, 2013. doi: 10.12720/ijsps.1.2.256-262. URL http://www.ijsps.com/uploadfile/2013/1128/20131128022014877.pdf.

Thiago Alencar and Karinna Matias. Bike fit e sua importancia no ciclismo. *Revista Movimenta*, 2(2), 2009. URL http://revistaseletronicas.pucrs.br/ojs/index.php/faenfi/article/viewFile/6145/4436.

M C Ashe, G C Scroop, P I Frisken, C a Amery, M a Wilkins, and K M Khan. Body position affects performance in untrained cyclists. *British journal of sports medicine*, 37:441–444, 2003. ISSN 0306-3674. doi: 10.1136/bjsm.37.5.441. URL https://www.ncbi.nlm.nih.gov/pmc/articles/PMC1751358/pdf/v037p00441.pdf.

C. Asplund and P. St Pierre. Knee pain and bicycling: fitting concepts for clinicians. *Phys Sportsmed*, 32 (4):23–30, 2004. doi: 10.3810/psm.2004.04.201. URL http://www.cyclocamping.com/articles/bicycle{_}knee{_}pain.pdf.

J. Balmer, R.C. Davison, and S.R. Bird. Peak power predicts performance power during an outdoor 16.1 km cycling time trial. *Medicine and Science in Sports and Exercise*, 32(8):1485–90, 2000. URL https://www.ncbi.nlm.nih.gov/pubmed/10949016.

E. Bergamini, P. Picerno, H. Pillet, F. Natta, P. Thoreuax, and V. Camomilla. Estimation of temporal parameters during sprint running using a trunk-mounted inertial measurement unit. *Journal of Biomechanics*, 45(6):1123 – 1126, 2012. doi: 10.1016/j.jbiomech.2011.12.020. URL http://www.sciencedirect.com/science/article/pii/S0021929012000176.

Rodrigo Bini, Patria A. Hume, and James L. Croft. Effects of bicycle saddle height on knee injury risk and cycling performance. *Sports Medicine*, 41(6):463–476, 2011. ISSN 01121642. doi: 10.2165/11588740-000000000-00000. URL https://link.springer.com/article/10.2165/11588740-000000000-00000.

C.V.C. Bouten, A.A. Sauren, M. Verduin, and J.D. Janssen. Effects of placement and orientation of body-fixed accelerometers on the assessment of energy expenditure during walking. *Medical and Biological engineering and Computing*, 35(1):50–56, 1997. doi: 10.1007/BF02510392.

E. R. Burke and A. L. Pruitt. Body positioning for cycling. In Human Kinetics, editor, *High-Tech cycling*, pages 69–92. 2 edition edition, 2003. ISBN 978-0736045070.

E.R. Burke. Perfect positioning. In *Serious cycling.*, pages 235–245. 2002. ISBN 978-0736041294.

Glen Cooper, Ian Sheret, Louise McMillian, Konstantinos Siliverdis, Ning Sha, Diana Hodgins, Laurence Kenney, and David Howard. Inertial sensor-based knee flexion/extension angle estimation. *Journal of Biomechanics*, 42:2678–2685, 2009. doi: 10.1016/j.jbiomech.2009.08.004.

Andrea Cutti, Alberto Ferrari, Pietro Garofalo, Michele Raggi, Angelo Cappello, and Adriano Ferrari. 'Outwalk': a protocol for clinical gait analysis based on inertial and magnetic sensors. *Medical and Biological engineering and Computing*, 48:17–25, 2010. doi: 10.1007/s11517-009-0545-x.

K. De Vey Mestdagh. Personal perspective: In search of an optimum cycling posture. *Applied Ergonomics*, 29(5):325–334, 1998. ISSN 00036870. doi: 10.1016/S0003-6870(97)00080-X. URL https://eurekamag.com/ftxt.php?pdf=009176718.

James Diebel. Representing Attitude : Euler Angles , Unit Quaternions , and Rotation Vectors. pages 1–35, 2006.

F. Diefenthaeler, R.R. Bini, and O. et al. Laitano. Assessment of the effects of saddle position on cyclists pedaling technique. *Medicine and Science in Sports and Exercise*, 38:181–82, 2006. doi: 10.1249/00005768-200605001-00821. URL https://www.researchgate.net/publication/216881184.

Fernando Diefenthaeler, Rodrigo Rico Bini, Ana Paula, and Barcellos Karolczak. Muscle activation during pedaling in different saddle position. *Revista Brasileira de Cineantropometria & Desempenho Humano*, 10, 2008. doi: 10.5007/1980-0037.2008v10n2p161. URL https://periodicos.ufsc.br/index.php/rbcdh/article/view/4160.

Nicholas J Dinsdale and Nicola J Dinsdale. Body position affects cycling comfort , performance , and overuse injury : A review of the relevance of discipline-specific body positions. *Journal of Sports Therapy*, 7(1):11–18, 2012.

S. Dorel, A. Couturier, and F. Hug. Influence of different racing positions on mechanical and electromyographic patterns during pedalling. *Scandinavian journal of medicine & science in sport*, 19(1):44–54, 2009. doi: 10.1111/j.1600-0838.2007.00765.x. URL https://www.ncbi.nlm.nih.gov/pubmed/18266790.

Hugo G. Espinosa, Jim Lee, Justin Keogh, Josie Grigg, and Daniel A. James. On the use of inertial sensors in educational engagement activities. *Procedia Engineering*, 112:262–266, 2015. ISSN 18777058. doi: 10.1016/j.proeng.2015.07.242. URL http://www.sciencedirect.com/science/article/pii/S187770581501499X.

E W Faria, D L Parker, and I E Faria. The science of cycling: factors affecting performance - part 2. *Sports Medicine*, 35(4):313–337, 2005. ISSN 01121642. URL http://physiovelo.com/wp-content/uploads/2016/11/The-Science-of-Cycling-Part-2-2.pdf.

J Favre, B M Jolles, R Aissaoui, and K Aminian. Ambulatory measurement of 3D knee joint angle. *Journal of Biomechanics*, 41:1029–1035, 2008. doi: 10.1016/j.jbiomech.2007.12.003.

J Favre, R Aissaoui, B M Jolles, J A De Guise, and K Aminian. Functional calibration procedure for 3D knee joint angle description using inertial sensors. *Journal of Biomechanics*, 42:2330–2335, 2009. doi: 10.1016/j.jbiomech.2009.06.025.

Daniel Tik Pui Fong and Yue Yan Chan. The use of wearable inertial motion sensors in human lower limb biomechanics studies: A systematic review. *Sensors (Switzerland)*, 10(12):11556–11565, 2010. ISSN 14248220. doi: 10.3390/s101211556. URL http://www.mdpi.com/1424-8220/10/12/11556/htm.

Magdalena Fronczek-wojciechowska, Karolina Kopacz, and Piotr Kosielski. Optoelectronic analysis of cyclists' position before and after a bike fit: A case study of a professional women's cycling team. *Trends in Sport Sciences*, 1(23):21–24, 2016. URL http://www.tss.awf.poznan.pl/files/2016/vol23no1/TSS{_}2016{_}123{_}3{_}21-24.pdf.

Samuel Fux, André Noth, Samir Bouabdallah, and Nikolic Janosch. *Development of a planar low cost Inertial Measurement Unit for UAVs and MAVs*. PhD thesis, 2008.

Carles Gomez, Joaquim Oller, and Josep Paradells. Overview and evaluation of bluetooth low energy: An emerging low-power wireless technology. *Sensors (Switzerland)*, 12(9):11734–11753, 2012. ISSN 14248220. doi: 10.3390/s120911734. URL http://www.mdpi.com/1424-8220/12/9/11734/htm.

E.J. Hamley and V. Thomas. Physiological and postural factors in the calibration of the bicycle ergometer. *The journal of physiology*, 191(2):55–56, 1967. URL https://www.ncbi.nlm.nih.gov/pubmed/6050117.

J.A. Hamley and T.D. Noakes. Peak power output predicts maximal oxygen uptake and performance time in trained cyclists. *European Journal of Applied Physiology and occupational physiology*, 65(1):79–83, 1992. URL https://www.ncbi.nlm.nih.gov/pubmed/1505544.

J.C. Holmes, A.L. Pruitt, and N.J. Whalen. Lower extremity overuse in bicycling. *Clinics in sports medicine*, 13(1):187–205, 1994. URL https://www.ncbi.nlm.nih.gov/pubmed/8111852.

Texas Instruments. CC2540 and CC2541 Bluetooth low energy Software Developer's. (September), 2015. URL http://www.ti.com/lit/ug/swru271g/swru271g.pdf.

Carolin Jakob, Patrick Kugler, Felix Hebenstreit, Samuel Reinfelder, Ulf Jensen, Matthias Lochmann, and Bjoern Eskofier. Estimation of the Knee Flexion-Extension Angle During Dynamic Sport Motions Using Body-worn Inertial Sensors. *Proceedings of the 8th International Conference on Body Area Networks*, pages 289–295, 2013. doi: 10.4108/icst.bodynets.2013.253613.

Tsolmonbaatar Khurelbaatar, Kyungsoo Kim, Su Kyoung Lee, and Yoon Hyuk Kim. Consistent accuracy in whole-body joint kinetics during gait using wearable inertial motion sensors and in-shoe pressure sensors. *Gait and Posture*, 42(1):65–69, 2015. ISSN 18792219. doi: 10.1016/j.gaitpost.2015.04.007. URL http://www.sciencedirect.com/science/article/pii/S0966636215004488?via=ihub.

Julio Francisco Kleinpaul, Luana Mann, Fernando Diefenthaeler, Antônio Renato, Pereira Moro, Felipe Pivetta Carpes, Centro De Desportos, Universidade Federal, De Santa Catarina, Centro De Ciências, and Universidade Federal. Aspectos determinantes do posicionamento corporal no ciclismo : uma revisão sistemática. pages 1013–1023, 2010. URL http://www.scielo.br/scielo.php?script=sci{_}arttext{&}pid=S1980-65742010000400022.

Frédéric Leens. An introduction to I2C and SPI protocols. *IEEE Instrumentation and Measurement Magazine*, 12(1):8–13, 2009. ISSN 10946969. doi: 10.1109/MIM.2009.4762946. URL http://ieeexplore.ieee.org/stamp/stamp.jsp?arnumber=4762946.

Gabriele Ligorio and Angelo Sabatini. Extended Kalman Filter-Based Methods for Pose Estimation Using Visual, Inertial and Magnetic Sensors: Comparative Analysis and Performance Evaluation. *Sensors*, 13(2):1919–1941, 2013. ISSN 1424-8220. doi: 10.3390/s130201919. URL http://www.mdpi.com/1424-8220/13/2/1919/htm.

Kun Liu, Tao Liu, Kyoko Shibata, and Yoshio Inoue. Ambulatory measurement and analysis of the lower limb 3D posture using wearable sensor system. *IEEE International Conference on Mechatronics and Automation*, pages 3065–3069, 2009. doi: 10.1109/ICMA.2009.5245982.

Kevin M. Lynch, Nicholas Marchuk, and Matthew L. Elwin. I2C Communication. In *Embedded Computing and Mechatronics with the PIC32 Microcontroller*, chapter Chapter 13, pages 191–211. 2016a. ISBN 9780124201651. doi: 10.1016/B978-0-12-420165-1.00011-1. URL http://linkinghub.elsevier.com/retrieve/pii/B9780124201651000111.

Kevin M. Lynch, Nicholas Marchuk, and Matthew L. Elwin. SPI Communication. In *Embedded Computing and Mechatronics with the PIC32 Microcontroller*, chapter Chapter 12, pages 177–190. 2016b. ISBN 9780124201651. doi: 10.1016/B978-0-12-420165-1.00012-3. URL http://linkinghub.elsevier.com/retrieve/pii/B9780124201651000123.

Ji Ma. Advanced MEMS Technologies and Displays. *Displays*, 37:2–10, 2015. doi: 10.1016/j.displa.2014.10.003. URL http://www.sciencedirect.com/science/article/pii/S0141938214000717.

P.W. Macdermid and A.M. Edwards. Influence of crank length on cycle ergometry performance of well-trained female cross-country mountain bike athletes. *European Journal of Applied Physiology*, 108(1):177–182, 2010. doi: 10.1007/s00421-009-1197-0. URL https://www.ncbi.nlm.nih.gov/pubmed/19771448.

K. Maenaka. MEMS inertial sensors and their applications. *5th International Conference on Networked Sensing Systems*, pages 71–73, 2008. doi: 10.1109/INSS.2008.4610859. URL http://ieeexplore.ieee.org/lpdocs/epic03/wrapper.htm?arnumber=4610859.

Antonio Maio. *Bluetooth Low Energy para Monitorização da Postura no Ciclismo*. PhD thesis, University of Minho, 2014. URL http://repositorium.sdum.uminho.pt/bitstream/1822/34095/1/Tese-AM-2014.pdf.

Nadim Maluf and Kirt Williams. *An Introduction to Microelectromechanical Systems Engineering*, volume 1. 2004. ISBN 9788578110796. doi: 10.1017/CBO9781107415324.004.

Raluca Marin-Perianu, Mihai Marin-Perianu, Paul Havinga, Simon Taylor, Rezaul Begg, Marimuthu Palaniswami, and David Rouffet. A performance analysis of a wireless body-area network monitoring system for professional cycling. *Personal and Ubiquitous Computing*, 17(1):197–209, 2013. ISSN 16174909. doi: 10.1007/s00779-011-0486-x. URL https://link.springer.com/article/10.1007/s00779-011-0486-x.

J.C. Martin and N.A. Brown. Joint-specific power production and fatigue during maximal cycling. *Journal of Biomechanics*, 42 (4):474–9, 2009. doi: 10.1016/j.jbiomech.2008.11.015. URL http://www.sciencedirect.com/science/article/pii/S0021929008006015.

Elisandro De Assis Martins, Frederico Dagnese, Julio Francisco Kleinpaul, Felipe Pivetta Carpes, and Carlos Bolli Mota. Evaluation of Body Position of Competitive and Recreational. *Revista Brasileira de Cineantropometria & Desempenho Humano*, 9(2):183–188, 2007. URL https://www.researchgate.net/publication/26460942.

Ruth E. Mayagoitia, Anand V. Nene, and Peter H. Veltink. Accelerometer and rate gyroscope measurement of kinematics: An inexpensive alternative to optical motion analysis systems. *Journal of Biomechanics*, 35(4):537–542, 2002. ISSN 00219290. doi: 10.1016/S0021-9290(01)00231-7. URL http://www.sciencedirect.com/science/article/pii/S0021929001002317.

Sanjeeb Mishra, Neeraj Kumar Singh, and Vijayakrishnan Rousseau. Sensor Interfaces. In *System on Chip Interfaces for Low Power Design*, chapter Chapter 10, pages 331–344. 1st editio edition, 2015. ISBN 978-0-12-801630-5. doi: 10.1016/B978-0-12-801630-5.00010-4.

G. Mornieux, JA Guenette, AW Sheel, and Et Al. Influence of cadence, power output and hypoxia on the joint moment distribution during cycling. *Journal of electromyography and kinesiology*, 20(1):102–107, 2007. doi: 10.1007/s00421-007-0555-z. URL https://link.springer.com/article/10.1007/s00421-007-0555-z.

Paul Myers. Interfacing using Serial Protocols Using SPI and I2C. Technical report, 2007. URL http://citeseerx.ist.psu.edu/viewdoc/download?doi=10.1.1.460.2531{&}rep=rep1{&}type=pdf.

Janosh Nikolic, Michael Bloesch, and Felix Renaut. MEMS Inertial Sensors Technology. 2013. URL http://students.asl.ethz.ch/upl{\protect\T1\textbraceleft}{_}{\protect\T1\textbraceright}pdf/383-report.pdf.

K.S. Nordeen-Snyder. The effect of bicycle seat height variation upon oxygen consumption and lower limb kinematics. *Medicine and sciences in sports*, 9(2):113–117, 1977. URL https://www.ncbi.nlm.nih.gov/pubmed/895427.

Karol J. O'Donovan, Roman Kamnik, Derek T. O'Keeffe, and Gerard M. Lyons. An inertial and magnetic sensor based technique for joint angle measurement. *Journal of Biomechanics*, 40: 2604–2611, 2007. doi: 10.1016/j.jbiomech.2006.12.010.

Sara Oliveira. *KneeRecovery: Rehabilitation Exercises for Knee Recovery at Home*. PhD thesis, 2017.

M. Patel and J. Wang. Applications, challenges, and prospective in emerging body area networking technologies. *IEEE Wireless Communications*, 17(1):80–88, 2010. doi: 10.1109/MWC.2010.5416354. URL http://ieeexplore.ieee.org/document/5416354/.

H. Peiwei. The Study on Swimming Exercises based on 3D Accelerometer Data Analysis. *International Journal of Advancements in Computing Technology*, 4(21):239–245, 2012. doi: 10.4156/ijact.vol4.issue21.28. URL https://www.researchgate.net/publication/272852955.

W. Peveler and J. Green. Effects of saddle height on economy and anaerobic power in well trained cyclists. *Journal of Strength and Conditioning Research*, 25(3):629–633, 2011. doi: 10.1519/JSC.0b013e3181d09e60. URL https://www.ncbi.nlm.nih.gov/pubmed/20581695.

Will W. Peveler. Effects of saddle height on economy in cycling. *Journal of Strength and Conditioning Research*, 22:1355–1359, 2008. doi: 10.1519/JSC.0b013e318173dac6. URL https://www.ncbi.nlm.nih.gov/pubmed/18545167.

Will W. Peveler, Josh D. Pounders, and Phillip A. Bishop. Effects of saddle height on anaerobic power production in cycling. *Journal of Strength and Conditioning Research*, 21:1023 – 1027, 2007. doi: 10.1519/R-20316.1. URL https://www.ncbi.nlm.nih.gov/pubmed/18076230.

W.W. Peveler, P. Bishop, J. Smith, M. Richardson, and E. Whitehorn. Comparing methods for setting saddle height in trained cyclists. *Journal of Exercise Physiology online*, 8:51–55, 2005. URL https://www.researchgate.net/publication/242268296.

Phillips Semicondutors. The I2C-Bus Specification, 2000. URL http://www.cs.unc.edu/{~}stc/FAQs/Interfaces/I2C-BusSpec-V2.1.pdf.

P. Picerno, V. Camomilla, and L. Capranica. Countermovement jump performance assessment using a wearable 3D inertial measurement unit. *Journal of Sports Sciences*, 29(2):139–146, 2011. doi: 10.1080/02640414.2010.523089. URL http://www.tandfonline.com/doi/full/10.1080/02640414.2010.523089?scroll=top{&}needAccess=true.

Pietro Picerno. 25 years of lower limb joint kinematics by using inertial and magnetic sensors: A review of methodological approaches. *Gait and Posture*, 5:239–246, 2017. doi: 10.1016/j.gaitpost.2016.11.008. URL http://dx.doi.org/10.1016/j.gaitpost.2016.11.008.

Pietro Picerno, Andrea Cereatti, and Aurelio Cappozzo. Joint kinematics estimate using wearable inertial and magnetic sensing modules. *Gait and Posture*, 28:588–595, 2008. doi: 10.1016/j.gaitpost.2008.04.003.

D. Price and B. Donne. Effect of variation in seat tube angle at different seat heights on submaximal cycling performance in man. *Journal of Sports sciences*, 15(4):395–402, 1997. doi: 10.1080/026404197367182. URL http://www.tandfonline.com/doi/abs/10.1080/026404197367182.

JW Ranklin and RR Neptune. Determination of the optimal seat position that maximizes average crank power: a theoretical study. *Proceedings of the North American Congress on Biomechanics*, 2008. URL http://archive.asbweb.org/conferences/2008/abstracts/485.pdf.

RF Digital Corp. Datasheet RFduino. Technical report, 2013.

A. D. Romig, Michael T. Dugger, and Paul J. McWhorter. Materials issues in microelectromechanical devices: Science, engineering, manufacturability and reliability. *Acta Materialia*, 51(19):5837–5866, 2003. ISSN 13596454. doi: 10.1016/S1359-6454(03)00440-3. URL http://www.sciencedirect.com/science/article/pii/S1359645403004403.

D.J. Sanderson and A.T. Amoroso. The influence of seat height on the mechanical function of the triceps surae muscles during steady-rate cycling. *Journal of electromyography and kinesiology*, 19(6):465–471, 2009. doi: 10.1016/j.jelekin.2008.09.011. URL http://www.sciencedirect.com/science/article/pii/S1050641108001442.

Julie L. Sauer, James J. Potter, Christine L. Weisshaar, Heidi Lynn Ploeg, and Darryl G. Thelen. Influence of gender, power, and hand position on pelvic motion during seated cycling. *Medicine and Science in Sports and Exercise*, 39(12):2204–2211, 2007. ISSN 01959131. doi: 10.1249/mss.0b013e3181568b66. URL https://www.ncbi.nlm.nih.gov/pubmed/18046192.

Hans H C M Savelberg, Ingrid G L Van de Port, and Paul J B Willems. Body Configuration in Cycling Affects Muscle Recruitment and Movement Pattern. *Journal of Applied Biomechanics*, 19(4):310–324, 2003. ISSN 10658483. doi: 10.1123/jab.19.4.310. URL http://journals.humankinetics.com/doi/abs/10.1123/jab.19.4.310.

Thomas Seel, Jorg Raisch, and Thomas Schauer. IMU-Based Joint Angle Measurement for Gait Analysis. 14:6891–6909, 2014. doi: 10.3390/s140406891.

Bosch Sensortec. BNO055 Datasheet. Technical report, 2014.

I Setuain, J Martinikorena, and M Gómez. Vertical jumping biomechanical evaluation through the use of an inertial sensor-based technology Vertical jumping biomechanical evaluation through the use of an inertial sensor-based technology. *Journal of Sports Sciences*, (August), 2015. doi: 10.1080/02640414.2015.1075057. URL https://www.ncbi.nlm.nih.gov/pubmed/26256752.

P.L. Shennum and H.A. DeVries. The effect of saddle height on oxygen consumption during bicycle ergometer work. *Medicine and Science in Sports*, 8(2):119–121, 1976. URL https://www.ncbi.nlm.nih.gov/pubmed/957931.

Matti Siekkinen, Markus Hiienkari, Jukka K Nurminen, and Johanna Nieminen. How Low Energy is Bluetooth Low Energy ? Comparative Measurements with ZigBee / 802 . 15 . 4. *IEEE Wireless Communications and Networking Conference Workshops*, pages 232–237, 2012. doi: 10.1109/WCNCW.2012.6215496. URL http://ieeexplore.ieee.org/document/6215496/.

M.R. Silberman, D. Webner, S. Collina, and B.J. Shiple. Road bicycle fit. *Clinical journal of sport medicine*, 15(4):271–6, 2005. URL https://www.ncbi.nlm.nih.gov/pubmed/16003043.

A.S.M. Silva. *Wearable sensors system for human motion analysis: Sports and Rehabilitation*. PhD thesis, Faculty of Engeneering of University of Porto, 2014. URL https://repositorio-aberto.up.pt/bitstream/10216/84342/2/33046.pdf.

Ming Sun and J.O. Hill. A method for measuring mechanical work and work efficiency during human activities. *Journal of Biomechanics*, 26(3):229–241, 1993.

Ryo Takeda, Shigeru Tadano, Akiko Natorigawa, Masahiro Todoh, and Satoshi Yoshinari. Gait posture estimation using wearable acceleration and gyro sensors. *Journal of Biomechanics*, 42: 2486–2494, 2009. doi: 10.1016/j.jbiomech.2009.07.016.

Toshiyo Tamura. Wearable Inertial Sensors and Their Applications. Number 1, pages 85–104. 2014. ISBN 978-0-12-418662-0. doi: 10.1016/B978-0-12-418662-0.00024-6. URL http://dx.doi.org/10.1016/B978-0-12-418662-0.00024-6.

M. Tanenhaus, D. Carhoun, T. Geis, E. Wan, and A. Holland. Miniature IMU/INS with optimally fused low drift MEMS gyro and accelerometers for applications in GPS-denied environments. *Position Location and Navigation Symposium (PLANS), 2012 IEEE/ION*, pages 259–264, 2012. doi: 10.1109/PLANS.2012.6236890. URL http://ieeexplore.ieee.org/document/6236890/.

Halim Tannous, Dan Istrate, Julien Sarrazin, Didier Gamet, and Tien Tuan Dao. A New Multi-Sensor Fusion Scheme to Improve the accuracy of knee flexion kinematics for functional rehabilitation movements.pdf. *Sensors*, 16, 2016. doi: 10.3390/s1611914.

Alessandro Tognetti, Federico Lorussi, Nicola Carbonaro, and Danilo De Rossi. Wearable Goniometer and Accelerometer Sensory Fusion for Knee Joint Angle Measurement in Daily Life. *Sensors*, 15:28435–28455, 2015. doi: 10.3390/s151128435.

Farid Touati, Rohan Tabish, and Adel Ben Mnaouer. A Real-time BLE Enabled ECG System for Remote Monitoring. *APCBEE Procedia*, 7:124–131, 2013. ISSN 22126708. doi: 10.1016/j.apcbee.2013.08.022. URL http://www.sciencedirect.com/science/article/pii/S2212670813001243.

T. Wanich, C. Hodgkins, J.A. Columbier, E. Muraski, and J.G. Kennedy. Cycling injuries of the lower extremity. *J Am Acad Orthop Surg*, 15:748–56, 2007. URL https://www.ncbi.nlm.nih.gov/pubmed/18063715.

E. Welbergen and L. Clijsen. The influence of body position on maximal performance in cycling. *European Journal of Applied Physiology*, pages 168–173, 1990. URL https://link.springer.com/article/10.1007/BF00236708.

Tim Wilmshurst and Rob Toulson. Starting with Serial Communication. In *Fast and Effective Embedded Systems Design*, chapter Chapter 7, pages 135–169. 2nd editio edition, 2016. ISBN 9780081008805.

T. Wishv-Roth. Assessment of cycling biomechanics to optimize performance and minimize injury. *Journal of Science and Medicine in Sport*, 2009. doi: 10.1016/j.jsams.2008.12.119. URL http://www.jsams.org/article/S1440-2440(08)00356-3/abstract.

H. Zhao and Z. Wang. Motion Measurement Using Inertial Sensors, Ultrasonic Sensors, and Magnetometers with Extended Kalman Filter for Data Fusion. *IEEE Sensors Journal*, 12 (5):943–953, 2012. ISSN 1530-437X. doi: 10.1109/JSEN.2011.2166066. URL http://ieeexplore.ieee.org/xpls/abs{_}all.jsp?arnumber=5999689.

Shengli Zhou, Qing Shan, Fei Fei, Wen J. Li, Chung Ping Kwong, Patrick Wu, Bojun Meng, Christina Chan, and Jay Liou. Gesture recognition for interactive controllers using MEMS motion sensors. *4th IEEE International Conference on Nano/Micro Engineered and Molecular Systems*, pages 935–940, 2009. doi: 10.1109/NEMS.2009.5068728.

R. Zhu and Z. Zhou. A real-time articulated human motion tracking using tri-axis inertial/magnetic sensors package. *IEEE Trans Neural Syst Rehabil Eng.*, 12:295–302, 2004. doi: 10.1109/TNSRE.2004.827825. URL https://nit.felk.cvut.cz/{~}dark/Petr/Jirka5/Pohyb/Clanky/01304870.pdf.